

REPORT DOCUMENTATION PAGE

Form Approved
OMB No. 0704-0188



AD-A266 656



Information is estimated to average 1 hour per response, including the time for reviewing instructions, searching existing data sources, and completing and reviewing the collection of information. Send comments regarding this burden estimate or any other aspect of this report for reducing this burden, to Washington Headquarters Services, Directorate for Information Operations and Reports, 1215 Jefferson Davis Highway, Suite 1204, Arlington, VA 22202-4302, and to the Office of Management and Budget, Paperwork Reduction Project (0704-0188), Washington, DC 20503.

1. REPORT DATE May 1993		3. REPORT TYPE AND DATES COVERED Final 15 May 88-14 May 91	
4. TITLE AND SUBTITLE New Vortex Dynamics Methods for Rotor Free Wake Analysis		5. FUNDING NUMBERS DAAL03-88-K-0062	
6. AUTHOR(S) Donald B. Bliss		8. PERFORMING ORGANIZATION REPORT NUMBER	
7. PERFORMING ORGANIZATION NAME(S) AND ADDRESS(ES) Duke University Durham, NC. 27708		10. SPONSORING/MONITORING AGENCY REPORT NUMBER ARO 25747.1-EG	
9. SPONSORING/MONITORING AGENCY NAME(S) AND ADDRESS(ES) U. S. Army Research Office P. O. Box 12211 Research Triangle Park, NC 27709-2211		11. SUPPLEMENTARY NOTES The view, opinions and/or findings contained in this report are those of the author(s) and should not be construed as an official Department of the Army position, policy, or decision, unless so designated by other documentation.	
12a. DISTRIBUTION/AVAILABILITY STATEMENT Approved for public release; distribution unlimited.		12b. DISTRIBUTION CODE	
13. ABSTRACT (Maximum 200 words) This report summarizes recent work on rotorcraft aerodynamics involving novel methods for rotor free wake calculations. A new method called Analytical/Numerical Matching (ANM) was developed. ANM is a hybrid analytical and numerical method that achieves accurate results by combining a low resolution numerical solution with a high resolution analytical solution. Although originally developed for vortex dynamics, ANM has proven to be of a general nature. The application of ANM to the rotor wake problem provides accurate answers with a significant reduction in computation time. The use of ANM introduces the opportunity to develop new solution strategies, including Far-Field Linearization and Periodic Inversion. These methods afford the means to obtain accurate solutions over the entire flight regime. Work involving applications of ANM has also led to a scheme that represents vortex filament dynamics by a hierarchy of nested problems of varying resolution joined by matching solutions. This approach, called ANM with Pyramiding (ANM/P), has reduced calculation times by more than a factor of twenty in some sample problems.			
14. SUBJECT TERMS Rotorcraft Aerodynamics, Vortex Dynamics, Free-Wake Analysis		15. NUMBER OF PAGES 51	
		16. PRICE CODE	
17. SECURITY CLASSIFICATION OF REPORT UNCLASSIFIED	18. SECURITY CLASSIFICATION OF THIS PAGE UNCLASSIFIED	19. SECURITY CLASSIFICATION OF ABSTRACT UNCLASSIFIED	20. LIMITATION OF ABSTRACT UL

DTIC
SELECTED
JUL 09 1993

New Vortex Dynamics Methods
for
Rotor Free Wake Analysis

DTIC QUALITY INSPECTED 5

Donald B. Bliss

May, 1993

Accession For	
NTIS CRA&I	<input checked="" type="checkbox"/>
DTIC TAB	<input type="checkbox"/>
Unannounced	<input type="checkbox"/>
Justification	
By	
Distribution /	
Availability Codes	
Dist	Avail and/or Special
A-1	

U. S. Army Research Office
ARO Grant: DAAL03-88-K-0062

Duke University

93 7 08 16 4

93-15582



5208

APPROVED FOR PUBLIC RELEASE;
DISTRIBUTION UNLIMITED

Foreword

An important research activity in aerodynamics involves the dynamics and stability of rotorcraft vortex wakes. This report summarizes recent work on rotorcraft aerodynamics involving novel methods for rotor free wake calculations. This research contributes to improved prediction of rotorcraft performance and vibratory loading in forward flight and in hover.

A new method called Analytical/Numerical Matching (ANM) was developed. ANM is a hybrid analytical and numerical method that achieves accurate results by combining a low resolution numerical solution with a high resolution analytical solution. ANM has some features in common with the method of matched asymptotic expansions. Although ANM was originally developed for a specific problem, the method has proven to be of a general nature. The initial application of ANM to the rotor wake problem shows the method to be accurate and to provide a significant reduction in computation time.

The use of ANM also introduces the opportunity to develop new solution strategies for free wake calculations, including Far-Field Linearization and Periodic Inversion. These methods afford the means to obtain accurate solutions over the entire flight regime, particularly in the difficult transition region between hover and low speed flight.

Finally, work involving applications of ANM has led to a scheme that represents vortex filament dynamics by a hierarchy of nested problems of varying resolution joined by matching solutions. This approach, called ANM with Pyramiding (ANM/P), has reduced calculation times by more than a factor of twenty in some sample problems.

Table of Contents

Foreword

Problem Statement

Summary of Important Results

List of Publications

List of Participants

Report on Inventions

References

Bibliography

Appendices A, B, and C.

Problem Statement

Free wake calculations which allow the wake vorticity field to evolve in free motion are the most accurate and physically correct approach to rotorcraft aerodynamics. From their inception, however, these calculations have faced difficulties, including the inadequacy of over simplified models of the wake, excessive computer time, questionable numerical accuracy, and convergence problems. As a result, ongoing research still has the objective of having free wake methods achieve their potential for rotorcraft engineering. However, there has been considerable recent progress. In particular, it is now apparent that a full-span computational treatment of the blade wake is necessary. Therefore, modern free wake analyses must deal with the motion of large, complete vorticity fields in order to be accurate.

The high resolution analysis of multi-blade, full-span free wakes of extended length is a significant challenge even for modern computational capabilities. In practice, there is a need to reduce the computer time of free wake calculations by at least one or two orders of magnitude. There is also a need to render free wake formulations more compatible with calculation methods for blade dynamics and aerodynamics. Finally, there is a need to explore free-wake methods that are not subject to instability in low speed flight and hover.

This research contract addressed the above issues and made significant improvements in the state-of-the-art by the development of novel new methods. The main subjects addressed were as follows:

- Development of Analytical/Numerical Matching (ANM), a new general approach to address numerical resolution and accuracy problems.
- Development of Far-Field Linearization, a method of simplifying far-field contributions in a rotorcraft wakes.
- Development of Periodic Inversion, a time independent quasi-linear procedure for evolving rotorcraft wake solutions.
- Development of Solution Pyramiding as an extension of ANM to greatly reduce computation time for a given problem size.

Each of these four important results are described in greater detail in the next section. Also, Appendices A, B, and C contain three relevant papers that have been presented on these subjects.

Summary of Important Results

Analytical/Numerical Matching

Analytical/Numerical Matching (ANM) is a hybrid technique that combines analytical and numerical solutions by a matching procedure. ANM allows a global low-resolution numerical solution and a local high-resolution analytical solution to be combined formally by asymptotic matching to construct an accurate composite solution. Both the numerical and analytical solutions are simpler and more easily obtained than the solution of the original problem, and the overall solution procedure is more efficient computationally than a direct approach to the original problem. In addition, the ANM approach has the ability to provide a high degree of spatial resolution in local areas without great computational burden.

Analytical/Numerical Matching was developed by Professor Donald Bliss at Duke University. The method has been applied to several problems in vortex dynamics, aerodynamics, and acoustics. These problems include: evaluation of the Biot-Savart integral for a vortex filament^{1,2}; the behavior of a vortex filament very near a surface^{3,4}; vortices cut by a rotor disk⁵; the roll-up of a two-dimensional vortex sheet⁶; an aerodynamic panel method⁷; and most recently to acoustic radiation and structural acoustic scattering⁸. In all these cases, very accurate solutions were obtained with a dramatic reduction in computational cost (factors of three to a hundred). Ongoing work considers the application of ANM to problems of unsteady compressible aerodynamics. Although, some new issues and difficulties may arise due to the propagating nature of solutions, there appears to be no fundamental reason why ANM cannot be applied to this case.

ANM is closely related to the method of Matched Asymptotic Expansions (MAE).^{9,10} MAE allows certain classes of problems having two disparate physical length scales to be divided into two simpler problems. The ratio of the two scales forms a small parameter. A series expansion is used to separate the problem into an "outer" problem, associated with the large scale, and an "inner" problem associated with the small scale. These problems are solved separately and combined using asymptotic matching to form a composite solution. The composite solution is the outer solution plus the inner solution minus the matching solution. The matching solution is the inner limit of the outer solution (or the outer limit of the inner solution). In the outer region the matching solution cancels the inner solution, whereas in the inner region it cancels the outer solution. The proper transition between regions requires an

"overlap" region, which will exist if the procedure is done correctly to an appropriate problem.

ANM is related to the method of Matched Asymptotic Expansions (MAE),^{9,10} but it differs in several important ways. The goal of ANM is to find an accurate solution to a physical problem having small scales or rapid variations that challenge the accuracy of the numerical method. In ANM, an artificial smoothing of the physical problem is introduced. The smoothing length scale must be larger than the scale associated with the numerical discretization, thereby assuring that the numerical solution of the smoothed problem is very accurate. However, the actual problem has a physical length scale smaller than the numerical discretization. The local region associated with the small scale is solved separately (usually analytically, but perhaps numerically) as an inner problem that captures the small scales and rapid variations. This inner problem, because of its idealizations, becomes increasingly invalid with increasing distance from the local region of rapid change.

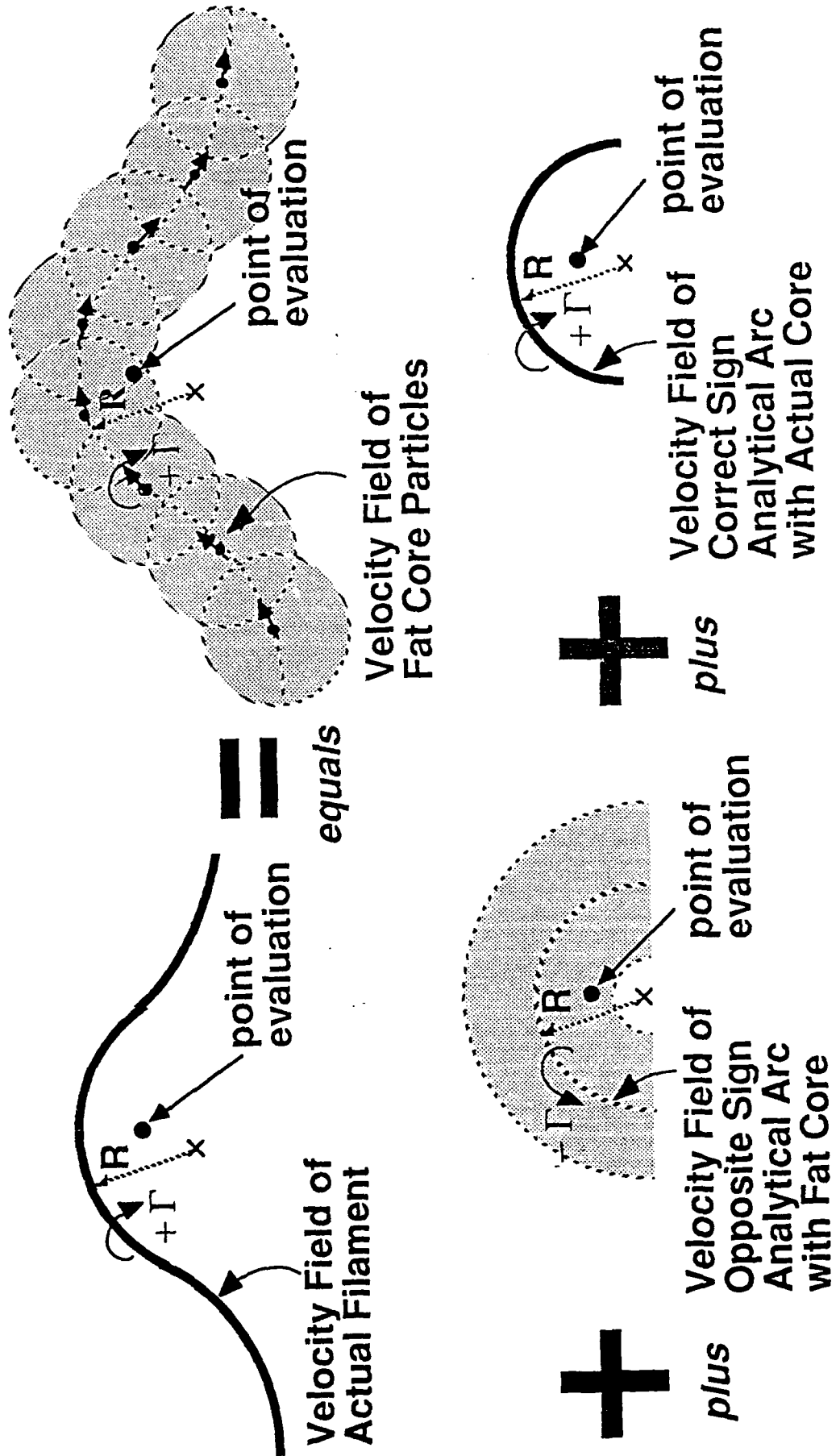
The numerical problem and the local problem are combined by asymptotic matching. This approach requires a matching solution that is similar to the inner problem but solved with the smoothing imposed. The composite solution is then given by the low-resolution global numerical solution plus the high resolution local solution minus the matching solution, namely:

$$\begin{aligned} \text{COMPOSITE SOLN.} &= \text{LOW RESOLUTION NUMERICAL SOLN.} \\ &+ \text{HIGH RESOLUTION LOCAL SOLN.} \\ &- \text{SMOOTHED LOCAL MATCHING SOLN.} \end{aligned}$$

In the local region, the matching solution subtracts away the local error associated with the smoothed numerical solution, leaving the local solution. Far from the local region, the local solution and the matching solution cancel, since they become identical beyond the smoothed region. For the method to work well, the smoothing must be chosen to achieve an overlap so that the transition zone between the local and numerical solutions is accurate.

The application of ANM to the calculation of a rotorcraft wake velocity field using the Biot-Savart law proceeds as follows (refer also to Figure 1). First, a low resolution numerical calculation of the velocity field is achieved by summing over discrete values of the Biot-Savart integrand, which is the simplest possible approximation of the Biot-Savart law. This approach is similar to the use of vortex particles or vortons, but the vortex particle formula is modified mathematically to produce a smoothing effect similar to a very large

FIG. 1. ANM COMPOSITE SOLUTION



(fat) vortex core. When summing the smoothed vortex particles, it can be shown that, if the cores of adjacent particles overlap slightly, the discrete numerical result accurately simulates a continuous fat core filament. This fact allows for the very efficient calculation of a smoothed fat core flow field by the simplest possible means. If taken alone, this result gives an accurate answer to the wrong problem because the core is too fat.

The solution can then be corrected analytically to remove the smoothing effect and restore the proper core structure. The local solution for the velocity field in the vicinity of a curve filament can be obtained analytically. At the point on the filament nearest the point of evaluation, two overlaid curved arc solutions are added to the numerical result. One solution consists of an arc with the correct core size and the other consists of a fat core arc with the opposite sign circulation.

Referring to Figure 1, for the portion of the filament nearest the point of evaluation, the opposite sign fat core arc cancels the fat core numerical solution in the nearfield, leaving the contribution of the arc with the correct core size. For the portion of the filament far away from the point of evaluation, and beyond the edge of the fat core, the two analytical arc solutions cancel each other leaving the numerical solution, which is correct at points beyond the fat core distance. The procedure to construct the solution in this case can be stated concisely as:

$$\begin{aligned} \text{COMPOSITE SOLN.} &= \text{FAT CORE NUMERICAL SOLN.} \\ &+ \text{ACTUAL CORE ANALYTICAL ARC SOLN.} \\ &- \text{FAT CORE ANALYTICAL ARC SOLN.} \end{aligned}$$

The detailed results presented in Appendices A and B show that this procedure, when properly implemented, leads to very accurate solutions with computation time reduced by approximately a factor of three. The reduction in computer time arises largely from the relative simplicity of the numerical solution, which is responsible for most of the computational burden. The analytical corrections are relatively simple, computationally inexpensive, and fairly easy to implement.

Far Field Linearization

A problem with traditional free wake methods is that a large amount of computer time is spent calculating the effect of vortex elements relatively far from the point of evaluation. The ANM approach described above provides a formal distinction between near-field and far-field effects.

In physical terms, the far field induces a smooth slowly varying velocity field on the point of evaluation, whereas the near field is associated with rapid changes and strong interactions. By the appropriate choice of scales, the numerical fat core free wake and the (opposite sign) fat core arc solution constitute the effective far-field solution by virtue of their smoothed, slowly varying nature. The analytical actual core arc solution, which is the remaining part of the composite solution, is entirely responsible for the strong, typically nonlinear, near-field effects. The fact that the near-field/far-field distinction arises naturally in the ANM method allows for the implementation of a formally correct procedure to perform partially linearized wake calculations.

The velocities induced by the far field are spatially linearized about some initial configuration using a truncated Taylor series in the wake position variables. As the wake evolves in time, the far-field velocities are approximated by evaluating the resulting linear expression, rather than recomputing the exact particle velocities from the Biot-Savart law. Note that this process involves only a matrix-vector multiplication. The linearized wake is re-used until the wake has evolved to the point where it is no longer accurate, at which time the wake is relinearized. Helicopters at moderate to high advance ratios have wakes that evolve relatively little, so that one linearization may suffice for an entire wake convergence calculation.

The linearized free-wake velocity problem takes the form of a large linear system (far field) with locally embedded nonlinearities (near field). Consistent with the matched asymptotic expansions approach of the ANM correction, the far field encompasses all of the vortex particles since their fat cores remove the strong near-field behavior. Furthermore, the fat and thin core components of the near-field ANM corrections may each be linearized. The highest accuracy results from computing the ANM corrections exactly at each time step, while the maximum efficiency is found by linearizing both the particles and the ANM correction, resulting in a complete linear description of the wake velocities. Between these extremes is the option of a linearized far field and a nonlinear near field. The completely linearized velocity expression also has the advantage of placing the wake velocities in a form functionally similar to the blade

dynamics problem, allowing the opportunity to solve these two aspects of the overall problem simultaneously in future work. Computer time comparisons for the various degrees of linearization are presented in Appendices A and B.

The use of vortex particles facilitates the analytical linearization of the wake velocities due to their simple functional form. Linearization of the ANM analytical nearfield correction is also possible, but with more effort due to the presence of elliptic integrals in their expressions. The closed-form derivation of the Taylor coefficients in the linearization were performed using a symbolic manipulation computer program. The velocity expressions are functions of 12 scalar variables for each element, and the derivative calculations are quite lengthy. Although the analytical formulation is more involved than a basic free wake method, the resulting savings in computer time more than justifies the approach.

Periodic Inversion

From their inception, free-wake calculations have been hampered by excessive computational effort and poor convergence behavior at low advance ratios and hover. Convergence in this context refers to the location of a wake structure which repeats every rotor revolution and is therefore steady state in a periodic sense. Indeed, because vortically induced velocity fields are inherently nonlinear, the existence of unique and stable solutions remains an open question. Thus it is not surprising that the time-marching approach to free-wake dynamics has encountered convergence difficulties.

Time-marching approaches begin with an assumed initial condition for the wake. As the integration proceeds, the errors in the initial wake are convected down and out of the free-wake as it relaxes to a converged configuration. Exact convergence is never reached by time marching, but is approached asymptotically. In high-speed flight, the time-marching approach converges without difficulty as the free stream convection dominates the solution, thereby reducing the strength and frequency of the strongly nonlinear near-field vortex encounters. However, in low-speed flight the free stream effect is reduced, resulting in a dense field of wake vorticity and the dominance of the strong near-field interactions.

Periodic Inversion is a new approach for the calculation of rotor free wakes that guarantees periodic steady-state solutions, and provides the means to solve for wake dynamics at all advance ratios, including low speed and hover. This is a unique capability since

traditional time-marching approaches fail at low advance ratios. The method is based on enforcing periodic boundary conditions over $1/B$ of a rotor revolution, where B is the number of blades. This is accomplished by defining a new set of wake variables with periodic behavior, and writing the governing equations in a linear perturbation form. The problem is written as a large linear system which is inverted for the perturbative correction. Successive iterations involving relinearization are required to obtain the final solution to the nonlinear problem.

The method of Periodic Inversion allows converged solutions to be found without the use of artificial damping, even at low advance ratios and hover. Performance curves are generated by varying the flight parameters between iterations. The method has been used to examine the low speed wake structure, which exhibits three unique forms depending on advance ratio: a helical structure from hover to some lower bound advance ratio, a roll-up structure above some higher bound advance ratio, and a rapid transition region between the two.

Periodic Inversion, which guarantees periodically steady-state solutions by enforcing periodic boundary conditions, is based on developing a system of collocation points with periodic behavior, as opposed to the Lagrangian description used in time-marching approaches. The vortically induced velocities determined from the Biot-Savart law are linearized, and the wake dynamics over a full period are written in a linear perturbation form. The Analytical/Numerical Matching (ANM) wake analysis is used to define the discrete wake model. The ANM model has been analytically linearized, as mentioned in the previous section, providing a basis for extension to Periodic Inversion. A new far-wake extension, which accounts for the semi-infinite domain of the wake, was also developed for this method and incorporated into the ANM model. The resulting problem takes the form of a large linear system of algebraic equations which is inverted for the perturbative correction vector. Because this is a linear approximation to a nonlinear problem, iterative refinement is typically required to reach convergence.

A primary advantage of Periodic Inversion is that it provides the means to study wake dynamics at all advance ratios, including hover. Low advance ratios have previously been unattainable for traditional time-marching approaches due to poor convergence behavior. The new method has shown that the wake maintains a roughly helical structure from hover up to some lower bound on the advance ratio. As the advance ratio is increased from this lower

bound through a narrow transition region, the wake quickly evolves into the familiar roll-up configuration characteristic of forward flight. At advance ratios above the transition region, the wake maintains the roll-up form and does not qualitatively change. Comparison with time-marching solutions show excellent agreement for wakes above the roll-up transition. Wakes within and below the transition region prove difficult for time-marching to converge, but there is evidence that the periodic solution provides a correct mean wake structure about which time-marching solutions oscillate.

Periodic Inversion also provides the means to generate performance curve data. Wake variables such as advance ratio, thrust coefficient and tip path plane angle can all be varied between iterations of the method. Points on a performance curve which are linearly close together can be incrementally found with one or very few iterations. This approach was used in the present study for two purposes. First, the wake was converged at hover by incrementing the thrust coefficient from 0.001 to 0.003. The thrust coefficient was then held constant as the advance ratio and tip path plane angle were increased. The pre- and post-transition range of the advance ratio were easily solved with a fairly large step size. Within the transition region, a much finer step size was required to capture the rapid change in the wake structure. The detailed results of this study are presented in Appendix C.

There are unique and promising opportunities for further extensions of the method. A generalization of the periodic variable description would allow the vortex element density to be increased in regions of strong vortex interactions, such as the advancing and retreating side roll up. This would result in a more efficient overall wake model without compromising accuracy. Coupling the wake dynamics with blade and body panel methods would allow an integrated approach to include both blade lift and interactinoal aerodynamics. This would result from the generalization of the linear system to include the lifting and non-lifting body panel equations. It appears possible to incorporate the blade dynamics into the method as well.

ANM with Solution Pyramiding

An extension of ANM has led to a scheme that represents vortex filament dynamics by a hierarchy of nested problems of varying resolution joined by matching solutions. This approach, called ANM with Pyramiding (ANM/P), has reduced calculation times by more than a factor of twenty in some sample problems.

The method was developed for predicting the dynamics of a system of free vortex particles ("vortons"), resulting in a new problem formulation with dramatically increased levels of computational efficiency over traditional methods. The combined solution approach, referred to as Analytical/Numerical Matching-Solution Pyramiding (ANM/P), capitalizes on the fact that many fluid dynamic structures may be decomposed into spatial near-field and far-field regions relative to a specified point of evaluation. The ANM/P technique breaks the problem into a hierarchy of associated problems which are easier and more efficient to solve than the original problem.

The resolution of vortex elements modeling a vortical flow field is governed by the accuracy required to capture the large velocity gradients in the spatial near-field. However, the bulk of the element calculations are in the far field, where the high resolution of the near field is unnecessary. The ANM methodology involves a low resolution far-field model that is combined with a high resolution near-field solution via a matching solution. Computationally, this composite solution is highly efficient without a significant loss of accuracy.

To further increase computational efficiency, the ANM methodology can be applied repeatedly to subdivide the domain of vortex elements into a series of nested problems. This procedure, known as Pyramiding, effectively produces a vorticity field composed of a hierarchy of centroidally grouped vortex elements of varying strength. This hierarchical structure minimizes the number of far-field calculations. Due to the matching nature of the ANM/P methodology, relatively little computation time is needed to define and index the various levels of centroidally grouped spatial domains. Typically, a large free vortex problem, such as a free rotor wake, will involve a flow field domain large enough to support multiple levels of pyramiding. Pyramiding reduces the computational problem from order N^2 to a problem approaching order N , where N is the number of vortex elements.

Although the approach developed here has been applied to vortex dynamics, it is broadly applicable to a wider range of problems in mathematical physics. A paper on ANM/P is in preparation, and a thesis on the subject has been completed (see the next section).

List of Publications

The first three papers listed below are appendices to this report.

"Vortex Filament Calculations by Analytical/Numerical Matching with Comparison to Other Element Methods", D. B. Bliss and W. O. Miller, presented at the AIAA 9th Computational Fluid Dynamics Conference, Buffalo, NY, June 14-16, 1989.

"Efficient Free Wake Calculations Using Analytical/Numerical Matching and Far-Field Linearization, D. B. Bliss and W. O. Miller, presented at the 45th Annual Forum of the American Helicopter Society, Boston, MA, May 1989.

"Direct Periodic Solutions of Rotor Free Wake Calculations by Inversion of a Linear Periodic System," D. B. Bliss and W. O. Miller, presented at the 46th Annual Forum of the American Helicopter Society, Washington, DC, May 1990.

"Vortex Dynamics Using Analytical/Numerical Matching (ANM) with Centroidal Grouping", D. B. Bliss and R. J. Epstein, manuscript in preparation for the AIAA Journal.

The following theses were prepared as part of this research activity.

"Analytical/Numerical Matching and Periodic Inversion: Two Advances in Free Wake Analysis," W. O. Miller, Ph.D Thesis, Department of Mechanical Engineering and Materials Science, Duke University, Durham, NC, 1990.

"Improved Efficiency in Free Vortex Problems Using Analytical/Numerical Matching and Solution Pyramiding," R. J. Epstein, MS Thesis, Department of Mechanical Engineering and Materials Science, Duke University, Durham, NC, 1991.

List of Participants

Principal Investigator: Professor Donald B. Bliss
Graduate Students: Wayne O. Miller, Ronald J. Epstein.

Report on Inventions

No patentable inventions were made under this contract.

References

1. "Efficient Free Wake Calculations Using Analytical/Numerical Matching and Far-Field Linearization", D. B. Bliss and W. O. Miller, Proc. of the 45th Annual Forum of the American Helicopter Society, Boston, MA, May 1989. Submitted to Vertica.
2. "Vortex Filament Calculations by Analytical/Numerical Matching with Comparison to Other Element Methods", D. B. Bliss and W. O. Miller, presented at the AIAA 9th Computational Fluid Dynamics Conference, Buffalo, NY, June 14-16, 1989.
3. "Free Wake Calculation of Rotor Flow Fields for Interactional Aerodynamics," T. R. Quackenbush and D. B. Bliss, Proc. of the 44th Annual Forum of the American Helicopter Society, Washington, DC, June 1988.
4. "Free Wake Calculation of Rotor Flow Fields for Interactional Aerodynamics," T. R. Quackenbush and D. B. Bliss, Vertica, Vol.14, No. 3, pp. 313-327, 1990.
5. "High Resolution Flow Field Prediction for Tail Rotor Aeroacoustics", T. R. Quackenbush, D. B. Bliss, and A. J. Mahajan, Proc. of the 45th Annual Forum of the American Helicopter Society, Boston, MA, May 1989.
6. "Vortex Dynamics Using Analytical/Numerical Matching (ANM) with Centroidal Grouping", D. B. Bliss and R. J. Epstein, manuscript in preparation for the AIAA Journal.
7. "An Aerodynamic Panel Method Based on Analytical/Numerical Matching", D. B. Bliss, and C. Castellino, manuscript in preparation for the AIAA Journal.
8. "Prediction of Acoustic Radiation Using Analytical/Numerical Matching," Bliss, D. B. and Peretti, L. F., presented at the 124th Mtg of the Acoustical Soc. Am., New Orleans, LA, Nov. 3, 1992.
9. Advanced Mathematical Methods for Scientists and Engineers, C. M. Bender and S. A. Orszag, McGraw-Hill, New York, 1978
10. Aerodynamics of Wings and Bodies, H. Ashley, and M. T. Landahl, Dover, New York, 1965.

Bibliography

The preceding references plus the reference lists of the papers in Appendices A, B, and C serve as the bibliography for this report.

Appendices

Appendix A:

"Vortex Filament Calculations by Analytical/Numerical Matching with Comparison to Other Element Methods", D. B. Bliss and W. O. Miller.

Appendix B:

"Efficient Free Wake Calculations Using Analytical/Numerical Matching and Far-Field Linearization, D. B. Bliss and W. O. Miller.

Appendix C:

"Direct Periodic Solutions of Rotor Free Wake Calculations by Inversion of a Linear Periodic System," W. O. Miller and D. B. Bliss.



AIAA 89-1962

**Vortex Filament Calculations by
Analytical/Numerical Matching
With Comparison to Other Methods**

D. B. Bliss and W. O. Miller

Duke University

Durham, NC

**AIAA 9th Computational Fluid
Dynamics Conference**

Buffalo, New York / June 13-15, 1989

Vortex Filament Calculations by Analytical/Numerical Matching With Comparison to Other Methods

Donald B. Bliss* and Wayne O. Miller**
Department of Mechanical Engineering and Materials Science
DUKE UNIVERSITY
Durham, North Carolina 27706

Abstract

The calculation of fluid velocity from the Biot-Savart law integrated over vortex filaments has traditionally been computationally expensive. Discretizing the filaments into N vortex elements results in order N^2 elemental velocity evaluations per time step. Further, the elemental resolution has been governed by the need to resolve the large velocity gradients in the near field of the filaments, resulting in unnecessarily high element densities in the far field, where the velocities are slowly varying. The method of Analytical/Numerical Matching (ANM) improves the efficiency of the filament velocity calculation without loss of near-field accuracy. This is done by using a far field comprised of computationally inexpensive vortex particles with a large core size for smoothing. The near field is done by an analytical correction which uses a thin physically correct core size to predict the large rapidly varying near-field velocities, and a second correction with the large core size to cancel the local vortex particle error and match to the far-field solution. As such, the ANM method is similar to the method of matched asymptotic expansions. The entire approach has been analytically linearized, which provides additional efficiency and allows unique solution opportunities. Examples are given which illustrate the efficiency and accuracy of the ANM method in vortex dynamics calculations.

Introduction

There are a number of problems in fluid mechanics and aerodynamics where the velocity field is constructed from the fluid vorticity field using the Biot-Savart law. Such cases often involve simulating the inviscid flow field from vortex wakes in free motion. An important application is the vortex wake of a helicopter rotor, and other examples include the trailing wakes of aircraft, shear layers, and the simulation of separated flows above swept wings. These cases involve the need to calculate the velocity field of curved, three-dimensional vortex filaments in an efficient and accurate manner.

Vortex filament calculations are solved numerically in Lagrangian coordinates by discretizing the filaments into piecewise segments, which are modeled by vortex elements. These elements represent the analytical integration of the Biot-Savart law for a short segment of the filament. Typically, straight-line or curved vortex elements have been used.¹ The filaments are followed

dynamically by tracing the evolution of the collocation points, markers on the filaments which are typically used as the endpoints or centerpoints of the elements. For free vortex motion, if there are N vortex elements, then to calculate the effect of each element on every other element requires N^2 element calculations. Grid assisted methods, such as the Cloud-In-Cell (CIC) technique typically reduce this to order $N \log(N)$ operations, but are not appropriate for general wake problems as they require periodic boundary conditions for efficiency.^{2,3,4} Furthermore, for problems that require convective washout of the initially assumed filament shape to converge to the correct answer, such as helicopter free wakes, the velocity calculations must be repeated order N times, resulting in a total of N^3 element calculations. The massive computational burden represented by such tasks quickly taxes even the fastest computers, and accuracy typically suffers as the element resolution must be reduced to pose a tractable problem. An important observation is that while the element resolution is governed by the required accuracy to capture the large gradient velocities in the local vicinity of a filament, or "near field", the bulk of the element calculations are in the "far field", where the high resolution required for the near field is wasted.

This paper describes a new approach to the vortex filament velocity calculation called Analytical/Numerical Matching (ANM). The ANM method provides high

Copyright © American Institute of Aeronautics and Astronautics, Inc., 1989. All rights reserved.

* Associate Professor, Mechanical Engineering, Duke University, Member AIAA.

** Doctoral Student, Mechanical Engineering, Duke University, Student Member AIAA.

accuracy but with substantial computational savings over previously used vortex element methods. In brief, the ANM method allows a low resolution far field model comprised of simple and efficient elements to be used for the majority of the velocity calculations. The strong near field velocities are captured by the addition of a local analytical correction that is applied only when appropriate. This analytical correction also serves as a mathematical matching of the far field and near field solutions. As such, the ANM method is similar to the method of matched asymptotic expansions. Further, the ANM approach has been analytically linearized to enhance the efficiency gains. Linearization allows the velocities to be determined by the simple evaluation of a perturbative linear system, rather than by recomputing the Biot-Savart velocities at each time step. Future work with linearization should also allow examination of the stability of various wake structures, such as those of helicopters in hover. Early experience with the ANM method has shown efficiency gains of better than five times over curved vortex elements without loss of accuracy, and an additional factor of two appears possible. By the addition of linearization, the efficiency gains increase to roughly twenty times over curved elements and further refinements are expected.

Vortex Filament Elements

Several vortex filament elements are in common use and will be described here. Specifically, the vortex particle, straight line vortex element and the Basic Curved Vortex Element (BCVE) will be discussed. Vortex particles, or "vortons", will be given particular emphasis as they form a basis for the ANM methodology. Vortex filament elements are appropriate for modeling potential flows with regions of concentrated vorticity. The obvious applications of filament elements are for cases where the vorticity is concentrated along space curves such as fully developed wing tip vortices, although vortex sheets and shear layers are also accurately modeled by a system of filament elements. Traditionally, sheets have been modeled by a grid or lattice of elements with varying strength, but a recent approach which is physically more consistent uses a contouring system of constant strength non-intersecting filaments. This is shown in Figure 1 where the full span wake of a helicopter rotor has been modeled by BCVE elements.⁵

Filament elements are based on the Biot-Savart law for vorticity along a curved line as given by Eq. 1.

$$\mathbf{v} = \frac{-\Gamma}{4\pi} \int \frac{\mathbf{r}_v \times d\mathbf{s}}{[r_v^2 + \epsilon^2]^{3/2}} \quad (1)$$

where r_v is the distance from the filament to the point of evaluation, and $d\mathbf{s}$ is the elemental filament length. The core radius parameter ϵ used by the authors effectively spreads the vorticity across a finite radius and removes the velocity singularity on the filament itself. This particular core treatment, in addition to being functionally simple, is also one of the earliest described

in the literature.⁶ The effect of the core radius on the swirl velocity about an infinite straight filament is shown in Figure 2. The velocity reaches a maximum at the core radius and smoothly reduces to zero at the filament center. At distances on the order of 2-3 core radii, the velocity quickly returns to that of a singular filament. As discussed below, a favorable effect of the core can be to spread the velocity field in such a way as to remove the discretization error associated with vortex particles.

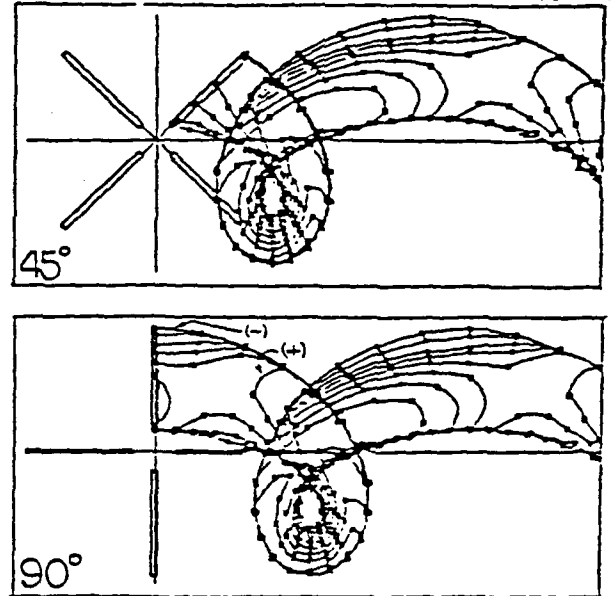


Figure 1. Two azimuthal positions of a full-span free wake of a four-bladed rotor modeled by vortex filament elements. Only one wake shown for clarity.

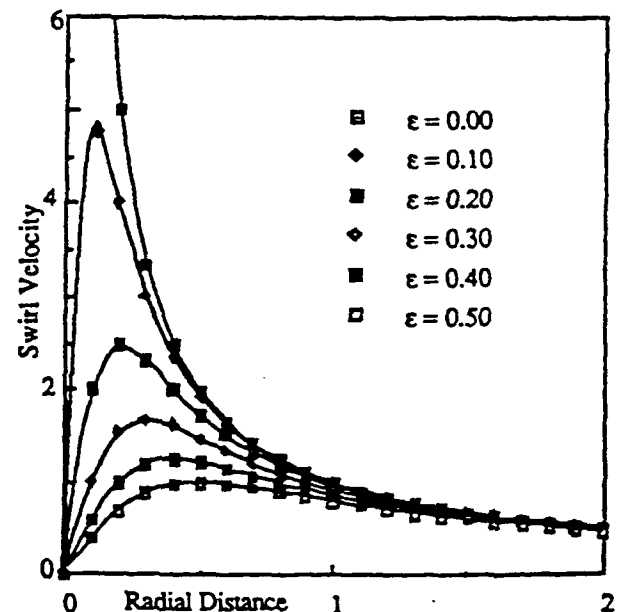


Figure 2. Effect of core radius ϵ on 2-D swirl velocity.

The vortex particle is the result of a simple discretization of the Biot-Savart law. The expression for

the velocity at a point induced by a filament vortex modeled with vortex particles is given by Eq. 2, where r_{vj} is the distance from the i th particle to the point of evaluation, and l_{sj} is the vector distance between the particles, essentially an effective element length (Fig. 3).

$$\mathbf{v} = \frac{-\Gamma}{4\pi} \sum_{i=1}^N \frac{\mathbf{r}_{vi} \times \mathbf{l}_{si}}{[r_{vi}^2 + \epsilon^2]^{3/2}} \quad (2)$$

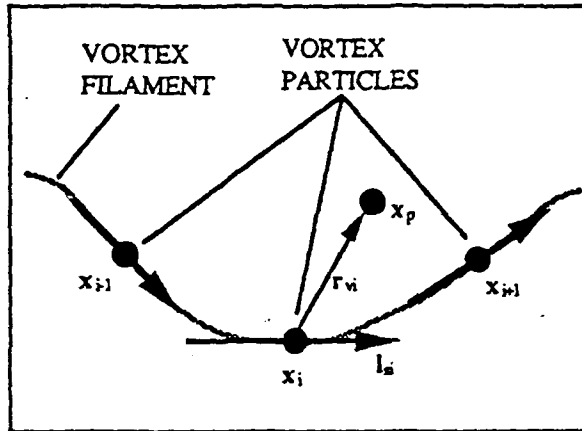


Figure 3. Geometry used for vortex particle evaluation.

The particle expression is both functionally simple and efficient to compute. Typically the particles are located coincident with the collocation points and tangent to the filament. The filament geometry is based on a local curve fit through neighboring collocation points on the filament. The discretization error of the velocity field obtained from vortex particles is based on the relative proximity to the filament and the core size used as illustrated in Figure 4, where vortex particles have been used to predict the swirl velocity of an infinite straight vortex filament. For a given radial distance from the filament, the discretization error appears as a lateral variation in the predicted velocity. As the core radius is increased this error is reduced and is negligible for core sizes on the order of one particle spacing. Thus the use of a suitably large core size results in a smooth and accurate velocity prediction for a filament with the same large core size. At distances greater than one particle spacing ($r/l_s > 1$), this error is seen to be less than 2% even without the core effect, indicating that vortex particles are highly accurate in the far field. At a distance of 2 to 3 particle spacings, the predicted velocity is essentially that of a filament without a core as the core effect decays rapidly with distance from the filament. Similar results are found for curved filament examples.

The straight-line vortex element is perhaps the most widely used element. It results from a piecewise linear fit to the vortex filament and is found by integrating the Biot-Savart law between the endpoints of the linear segments (Fig. 5). The velocity due to a single element is given in Eq. 3, where a local cylindrical coordinate system is used. This expression is

more complicated and computationally expensive than the corresponding vortex particle velocity expression.

$$\mathbf{v} = \frac{\Gamma}{4\pi r} \left\{ \frac{x + \frac{l_s}{2}}{\sqrt{(x + \frac{l_s}{2})^2 + r^2}} - \frac{x - \frac{l_s}{2}}{\sqrt{(x - \frac{l_s}{2})^2 + r^2}} \right\} \mathbf{e}_\theta \quad (3)$$

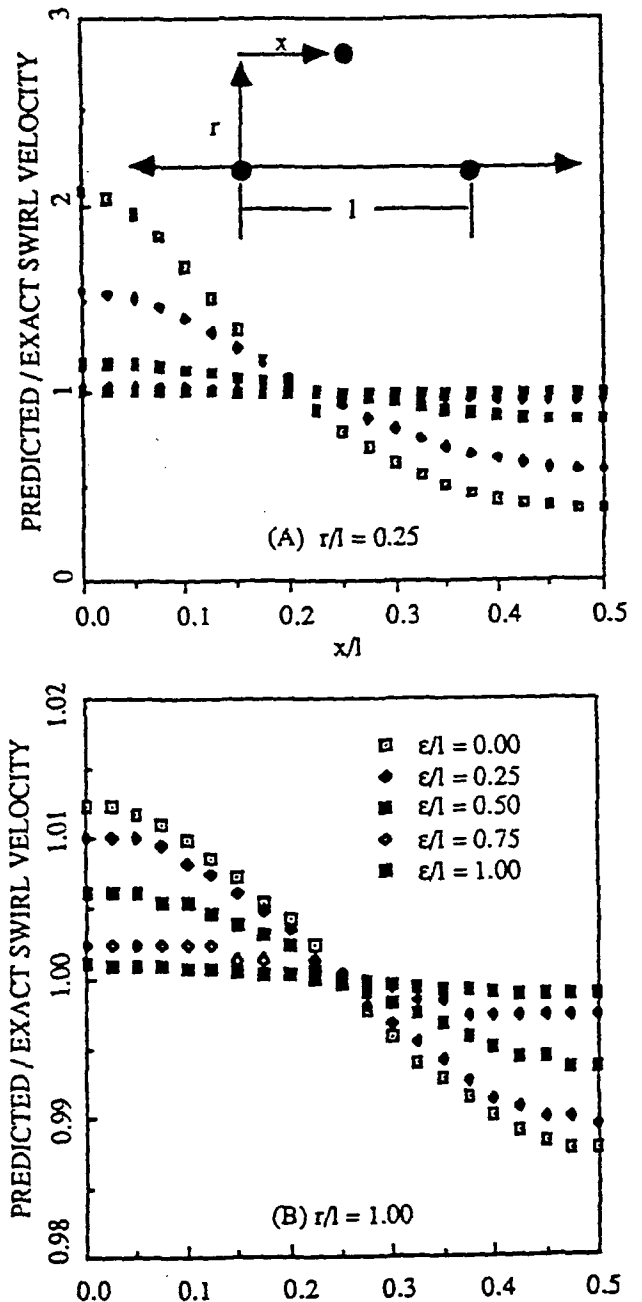


Figure 4. Effect of core size on the discretization error as a function of lateral distance between vortex particles. (A) Radial distance = 0.25 element spacing. (B) Radial distance = 1.00 element spacing. Note vertical scales.

The elemental errors are of two types, position errors and curvature errors. Position errors arise because the straight-line elements do not coincide with the filament position at most points along the curve. Curvature errors arise from the failure to duplicate the local curvature of the filament. The effect of curvature on filaments of infinitesimal cross section is to produce a binormal velocity component that depends logarithmically on the distance from the filament, and is singular on the filament.⁷ For filaments of finite cross section (non-zero core size), this results in a finite self-induced filament velocity. A detailed study of the errors associated with both straight line and curved vortex elements is given in Reference 1. As with the vortex particle, the errors are local in scope so that at distances greater than an element length the results are accurate.

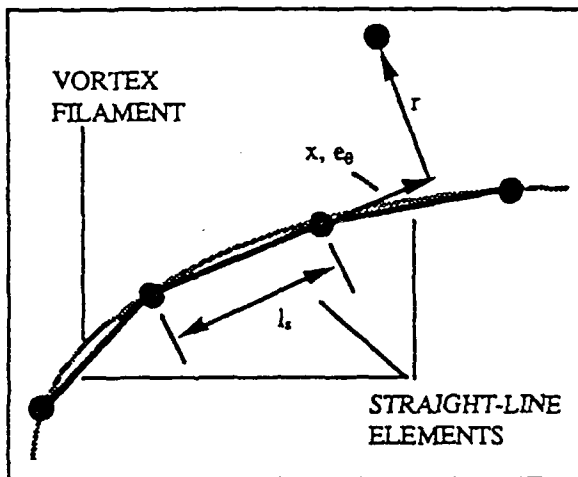


Figure 5. Local coordinate geometry used for straight-line element evaluation.

The Basic Curved Vortex Element (BCVE) is a relatively recent element model which has proven to be very accurate.^{1,8,9,10} It is based on a local parabolic fit to the filament (Fig. 6) and thus includes the effects of curvature while reducing positional errors as well. The elemental velocity contribution requires the evaluation of three related integrals as given by Eq. 4, where the coefficients c_n depend on the strength and curvature of the BCVE, and on the relative position of the evaluation point.

$$v = \sum_{n=0}^3 c_n I_n, \quad I_n = \int_{BCVE} \frac{x^n dx}{[a + bx + cx^2]^{3/2}} \quad (4)$$

The high accuracy and good local fit of the BCVE allow many fewer elements to be used to model a filament shape to good accuracy. The relative complexity of the velocity expression makes the element more expensive to use however: experience has shown that the BCVE is roughly twice as expensive as the straight line element, and 5-10 times more expensive than vortex particles. The relative cost of the BCVE has

been justified in the past by the need to accurately predict the strong nonlinear interactions of close filament encounters. This has been of particular importance for modeling helicopter wakes, where high resolution of the wake is necessary for accurate blade load predictions.^{5,11}

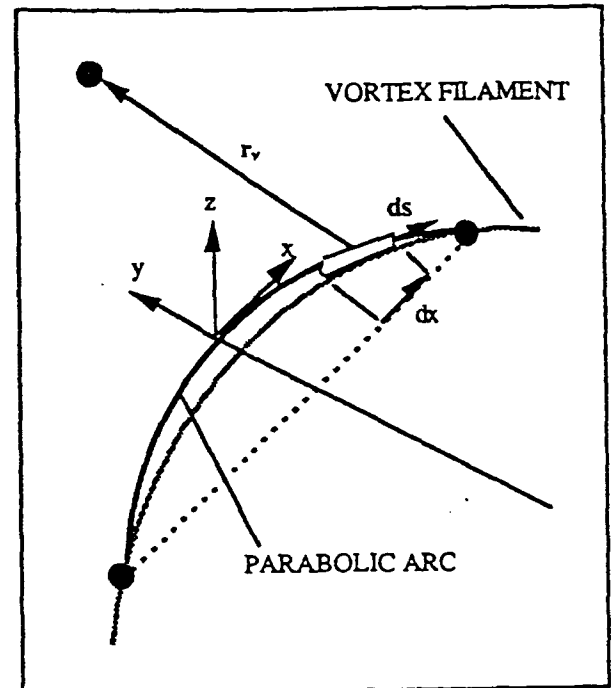


Figure 6. BCVE parabolic element fit to vortex filament.

Analytical/Numerical Matching

The Analytical/Numerical Matching, or ANM, methodology is based on the observation that many practical wake structures may be conceptually decomposed into a near-field and a far-field region relative to a point of evaluation as suggested in Figure 7. The near field is in the immediate vicinity of a vortex filament and is defined by strong nonlinear induced velocities with large gradients. The far field comprises the rest of the wake and is characterized by small slowly varying induced velocities. In traditional practice the overall element resolution is governed by the need to resolve the near field with sufficient accuracy. This is highly inefficient as the near field consists of only a few of the elements. The bulk of the elements, which are in the far field, are an unnecessary computational burden as the far field can be accurately resolved with many fewer elements. As the computational effort goes as the square of the number of elements, the unnecessary elements quickly overwhelm the velocity calculation.

The ANM approach addresses this issue of accuracy versus efficiency by accurately resolving the near-field interactions while using a low resolution far field. The far field is modeled by relatively few of the computationally inexpensive vortex particles, which are very accurate in the far field. The near field is done by an exact analytical result for a curve that locally coincides

with the filament. The analytical correction is applied only as needed for near-field interactions, and accurately captures the strong local velocities near the vortex filament. In particular, the ANM approach has three components: a far field comprised of vortex particles with a large, typically nonphysical, core size, a near-field correction with the physically correct core size, and a second near-field correction of opposite sign with the fat core size that is used to match the particle and analytical solutions (Fig. 8). The approach is similar to the method of matched asymptotic expansions, where the fat core particle solution is analogous to the outer solution, the thin core analytical solution is like the inner solution, and the opposite sign fat core analytical solution acts as the matching solution.

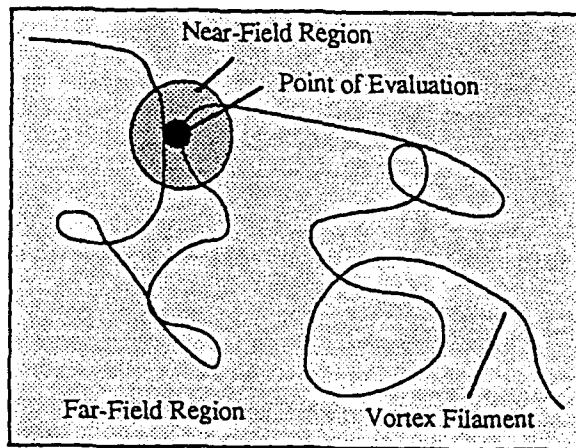


Figure 7. Distinction of small high velocity gradient near field embedded in a low gradient far field.

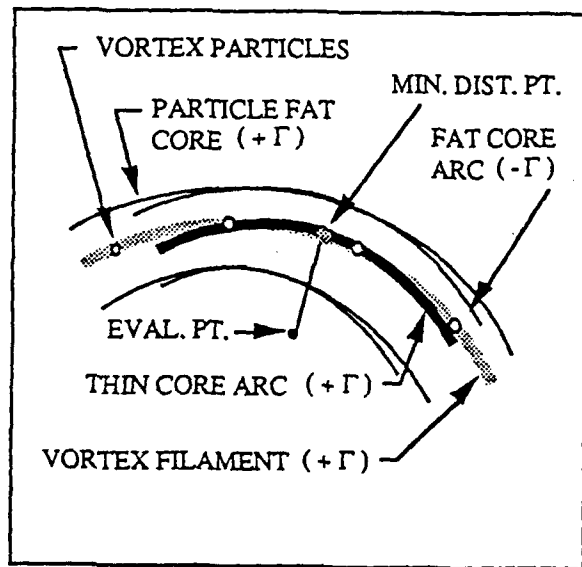


Figure 8. Three-part ANM composite solution: (1) fat core vortex particle outer solution, (2) thin core analytical inner solution, and (3) opposite sign fat core analytical matching solution.

The outer far-field solution from the fat core vortex particles encompasses the entire wake structure, being present even in the spatial near field. This is possible because the core size is chosen large enough to remove the steep velocity gradients near the filament. As previously discussed, the fat core also removes the discretization error of the low resolution particle model. The outer solution thus represents a smooth and accurate solution to a filament with the same large core size. While not physically accurate near the filament, where the actual velocities are large, the outer solution is valid at distances on the order of the particle spacing. The inner near-field solution of the thin core analytical correction is accurate locally as the curve fit is very good near the evaluation point. The thin (physical) core used also captures the physically correct large local velocity gradients. The inner solution degrades in accuracy with distance from the filament as the curve used for the correction is no longer accurately fit to the filament. The matching solution of the opposite-sign fat core analytical correction provides the transition between the inner and the outer solutions. In the spatial far field, the thin and fat core analytical corrections cancel each other, leaving the outer particle solution. This cancellation is due to the local effect of the core and to coincident curve fits used for both analytical corrections. In the near field, the fat core particle solution and the fat core analytical solution cancel, leaving the thin core analytical solution. The near field cancellation is a result of the small smooth velocities predicted by both fat core solutions at distances within a core radius. At intermediate distances (e.g. one particle spacing), the matching solution provides a smooth transition between the inner and outer solutions.

The analytical correction used in conjunction with the vortex particles may be based on any curve geometry that allows a tractable solution of the Biot-Savart integral. The development given here is for a closed circular ring, although a previous effort successfully used a parabolic arc. The ring is based on the filament geometry at the point of minimum distance from the evaluation point (Fig. 9). The local radius of curvature is used, and the ring is located in the local plane of curvature. The Biot-Savart integral with the core radius (Eq. 1) may be solved in closed form for this geometry, and the resulting normal and binormal velocities are given in Eqs. 5-7, where v_n and v_b are the ring normal and binormal velocities respectively, and k is the elliptic modulus.

$$v_n = \frac{-\Gamma R z}{\pi [r^2 + \epsilon^2]^{3/2}} \left\{ \sqrt{1-k^2} E(k) - \frac{2[1-k^2]^{3/2}}{k^2} (K(k) - E(k)) \right\} \quad (5)$$

$$v_b = \frac{-\Gamma R (R+x)}{\pi [r^2 + \epsilon^2]^{3/2}} \left\{ \frac{2[1-k^2]^{3/2}}{k^2} (K(k) - E(k)) \right\} + \frac{\Gamma R x}{\pi [r^2 + \epsilon^2]^{3/2}} \left\{ \sqrt{1-k^2} E(k) \right\} \quad (6)$$

$$k^2 = \frac{4R(R+x)}{r^2 + \epsilon^2 + 4R(R+x)} \quad (7)$$

The complete elliptic integrals $E(k)$ and $K(k)$ are evaluated efficiently by the use of simple polynomial expressions with the proper logarithmic behavior.¹² The limiting behavior of the ring solution provides the proper self-induced velocity for a finite core filament, so that the solution is valid for all local evaluation points, including the collocation points themselves.

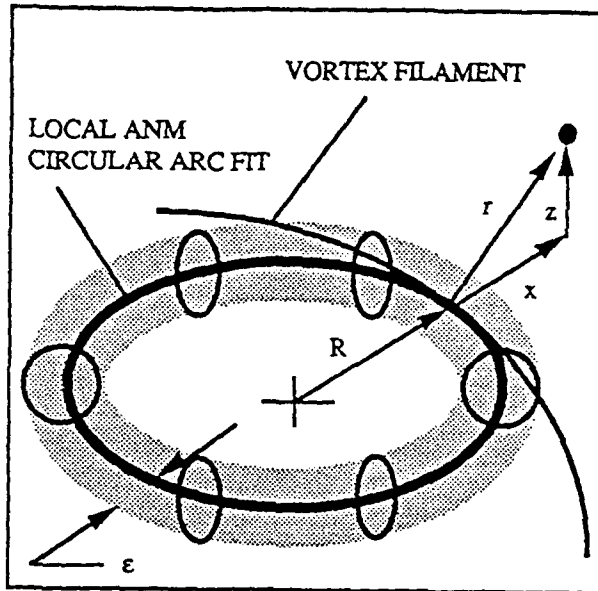


Figure 9. ANM correction arc geometry based on circular ring fit to local filament geometry.

Velocity Linearization

One justification of the ANM methodology was that the near field of a vortex filament is characterized by a strong, rapidly varying velocity field which cannot be accurately described by vortex particles alone. By the same argument, the far field is characterized by a relatively weak and slowly varying velocity field, and these properties make the far field a candidate for linearization. The velocities induced by the far field are spatially linearized about some initial filament configuration using a truncated Taylor series in the collocation point position variables. As the filament positions evolve in time, the far-field velocities are approximated by evaluating the resulting linear expression, rather than by recomputing the exact particle velocities from the Biot-Savart law. The Taylor coefficients are re-used until the filaments have evolved to a point where the coefficients are no longer valid, at which point they may be recomputed. Many practical applications may be accurately modeled with only a single linearization as the filaments may evolve relatively little over the course of a computational run. An important example is the wake of a helicopter rotor at high advance ratio (fast forward flight).

Linearization may be partial or complete to provide several levels of efficiency and accuracy. Of course, the highest accuracy results from computing all three of the ANM velocity components at each time step without any linearization. The highest efficiency results from linearizing all three of the ANM velocity components, resulting in a completely linearized velocity expression. Between these extremes is the option of a linearized far field and a (functionally) nonlinear near field. The choice of which approach to take depends on the problem being solved, especially on the rate of filament evolution and the importance of near-field interactions. The linearized velocity problem may then take the form of a large linear system (far field) with locally embedded nonlinearities (near field). Consistent with the mathematical matching approach of the ANM method, the far field encompasses all of the vortex particles plus the analytical fat core arc since their fat cores remove the strong near field behavior. Furthermore, the thin core component of the analytical correction may also be linearized for the fully linearized case.

Linearization also allows new solution strategies to be considered. One approach under consideration finds periodic solutions of rotor wakes directly by inversion of a linear system derived from the linearized wake velocities.¹³ Note that the linear system does not need inversion for typical time marching integration as the perturbation distances are known in advance. Future work with the fully linearized velocities will include examination of the stability of wake structures by means of the eigenvalues of the coefficient matrix. This will be especially interesting for the cases of helicopter wakes in hover and transitional flight, as they have often proved difficult to converge, and may well exhibit chaotic behavior.

As presented here, the geometries of the vortex particles and the analytical corrections are based on 3-point circular arcs passed through the particle and its two adjacent neighbors. The individual velocity expressions are functionally dependent on the three points and on the point of evaluation, resulting in 12 scalar variables. The linearized expression may be expressed as in Eq. 8, where g_k are the individual scalar position variables.

$$v = v_0 + \sum_{k=1}^{12} \frac{\partial v}{\partial g_k} \Delta g_k \quad (8)$$

$$g_k \in \{x_{i-1}, y_{i-1}, z_{i-1}, x_i, y_i, z_i, x_{i+1}, y_{i+1}, z_{i+1}, x_p, y_p, z_p\}$$

When the velocity expressions given by Eqs. 2 and 5-7 are written in their full functional form, they present a daunting task to linearize. Rather than attempt the Taylor expansion by hand, the coefficients were found by using SMP, a symbolic manipulation computer program similar to MACSYMA and Mathematica. The use of SMP greatly reduced the chance of human error in these calculations, and subsequent code verification proved the derivatives to be

correct. The program was also used to translate the resulting symbolic output directly into FORTRAN source code.

Results and Comparisons

Several evaluation problems have been used to examine the accuracy and efficiency of the ANM method. To begin, the work done in Reference 1 comparing the accuracy of the straight line and BCVE elements was extended to include both vortex particles and the full ANM method. Typical results are given in Figure 10 which presents the error in the normal velocity component w directly above a vortex ring of infinitesimal cross section (zero core size). Here end points, quarter points and mid points refer to relative positions above the vortex elements. It is surprising to note that the simple vortex particle gives better accuracy than the straight line element for all proximities, and is better by a full order of magnitude at a distance of one element spacing ($r/l_s = 1$). The ANM correction results in excellent accuracy which surpasses that of the BCVE in the filament near field. The error is due to the slight residual from the cancellation of the fat core particle outer solution and the fat core analytical matching solution. The ANM data was generated using a fat core size equal to the particle spacing, and a thin core size equal to zero.

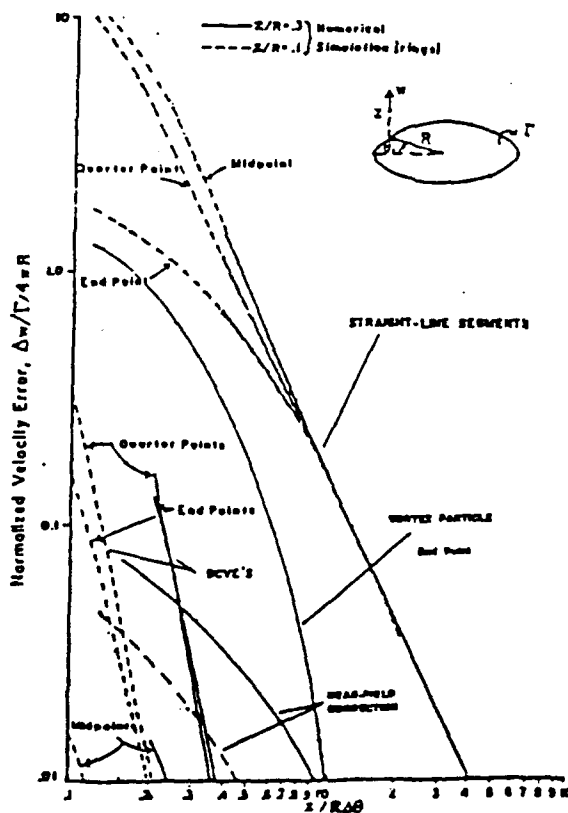


Figure 10. Errors in vertical velocity above a vortex ring as predicted by the ANM near-field correction, BCVE elements, vortex particles, and straight-line elements. Element spacing $l_s = R \Delta\theta$.

Recall that for N elements, the number of elemental velocity evaluations for a single filament calculation goes as N^2 . Additional computational efforts require order N and order 1 calculations. By fitting the CPU time to a quadratic polynomial in N , the relative elemental efficiencies can be compared by looking at the quadratic coefficient. These data are given in Figure 11, where the coefficients have been normalized to the BCVE element. The ANM method is 3.4 times faster than the BCVE, and the particles are 5.9 times faster. Typical filament velocity calculations would primarily use particles, with a much smaller number of the ANM near field corrections, resulting in an overall efficiency gain of roughly 5 or better. These numbers are based on a code developed in local coordinates, with the overhead of the coordinate transformations. There is evidence that a code re-worked in global coordinates would double the efficiency gains, resulting in an overall efficiency gain of an order of magnitude over the BCVE. Also shown are the linearization efficiencies. The time to analytically linearize the complete ANM correction is 1.4 times that of a BCVE velocity calculation. It includes the ANM velocity calculation and the Taylor coefficient evaluations. Once the linearization is done, the time to evaluate the resulting linear velocity expression is given as 0.06 times a BCVE calculation, or roughly a gain of 20. The efficiency runs were made on a SUN-4 computer, which is a traditional scalar processor. Vector machines such as Cray and CONVEX would substantially improve the linearization evaluation gains as it is simply a matrix-vector multiplication with a vector addition (e.g. $Ax + b$).

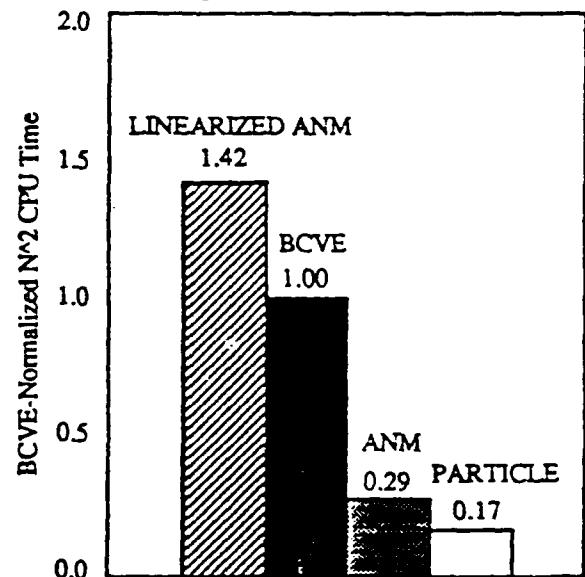


Figure 11. Computational efficiency for N^2 operations normalized to the BCVE element (N = number of vortex elements).

The ability of the ANM method to correct the particle discretization error is shown in Figure 12. A vortex ring was modeled with 12 particles at 30° azimuthal spacing, and the normal velocity in the ring

plane was computed along radii which intersected the ring at several relative locations between the particles. Figure 12(A) shows that the uncorrected particles exhibit substantial variation in the near-field velocities as the radial azimuth was varied. For this example the particles were given a small core size to reduce the smoothing effect. The same positions are shown in Figure 12(B), but with the addition of the ANM near field correction. The corrected velocities at all azimuthal angles are in excellent agreement with the analytical result.

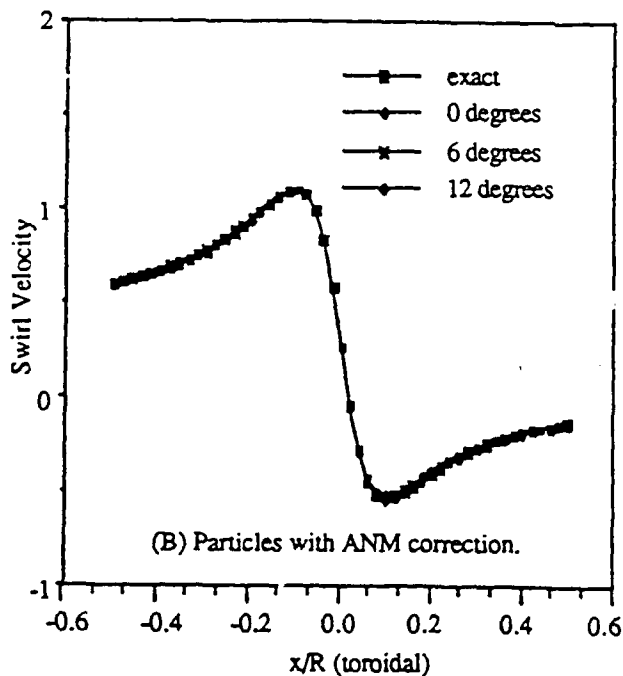
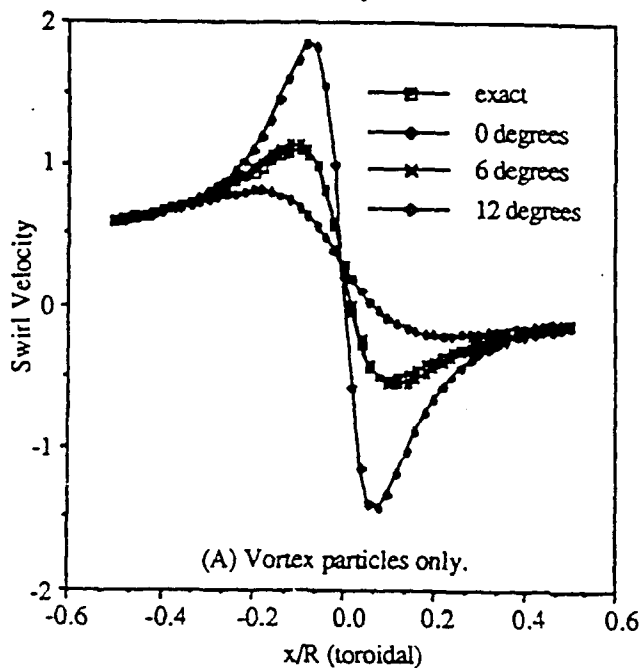


Figure 12. Vortex ring swirl velocity along radii of varying azimuthal angles measured between collocation points: (A) Vortex particles alone. (B) Particles with the ANM near-field correction applied

A similar example was done for an ellipse with a 4:1 axis ratio to examine the ANM accuracy for non-circular geometries. Figure 13 presents the normal velocities evaluated along the major axis as the fat core size varies from half to twice the local element spacing.

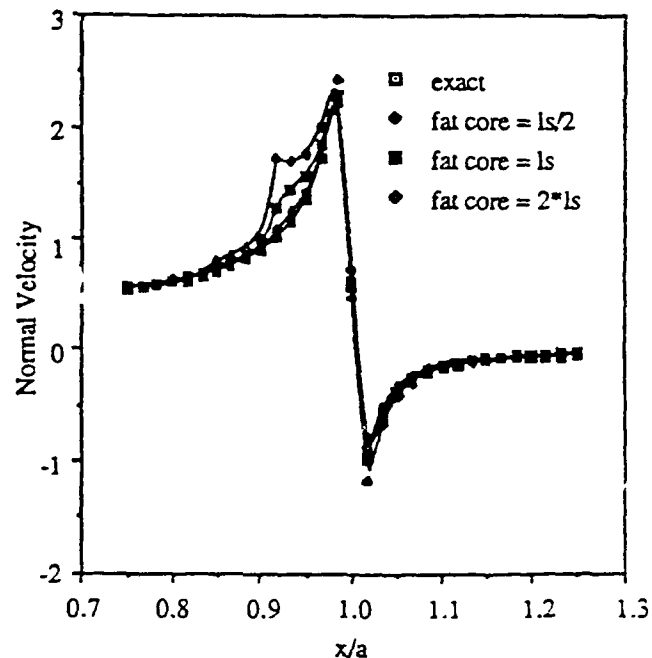


Figure 13. Normal velocities in the plane of a 4:1 ellipse (major axis length $a = 4$) predicted by the ANM method at distances near the fat core radii. Element spacing = l_s .

The larger fat core results are seen to overpredict the velocity near the filament in the ellipse interior. There are two combined mechanisms responsible for this. First, the overpredicted evaluation points project to two local minima on the ellipse, which are very close together as this is near a major vertex. As a result, two ANM corrections are applied in close proximity to each other. This case may be expected to occur in practice as filaments may be highly curved near an evaluation point due to a tendency to intertwine and roll up. Second, the evaluation points lie near or within the larger core radii, placing them in the near field of both minima. Also, the larger fat cores shown are 4 and 8 times bigger than the (physical) thin core, resulting in non-negligible residuals from the cancellation of the fat and thin core analytical solutions at this distance. The residuals would be correctly canceled by the fat core particle solution if the evaluation points were within only one near-field region. However, the presence of two overlapping near fields results in an additional residual velocity that is not canceled, but incorrectly added to the predicted velocity thus accounting for the overprediction error. The smallest fat core does not exhibit this problem as the evaluation points with two minima lie well outside the near field radius. This shows that as the fat core size approaches the thin core size, the residual is reduced and

the above problem becomes less serious. Thus the choice of the fat core size is not arbitrary: it must be small enough to avoid this extra residual problem (typically less than the expected minimum radius of curvature of the filament), while being large enough to smooth the particle solution to avoid discretization error. The important point is that the fat core size must be chosen appropriately to achieve a proper mathematical overlap in the composite solution matching.

As a practical application, the ANM methodology was incorporated into a helicopter free wake program.¹³ Helicopter wakes present a demanding test due to the strong near field interactions found in the roll up of the wake on the advancing and retreating sides. Figure 14 presents a wake from a single-bladed helicopter flying at low forward speed (0.1 advance ratio). The wake was converged from an initial assumed wake with a simple skewed helix geometry to the convoluted roll-up shown which is typical of low speed flight. The far field was linearized and the near field used the full ANM correction. The roll-up was captured with the very low element density of 12 per rotor revolution. An identical run using the BCVE elements resulted in a nearly identical wake structure.

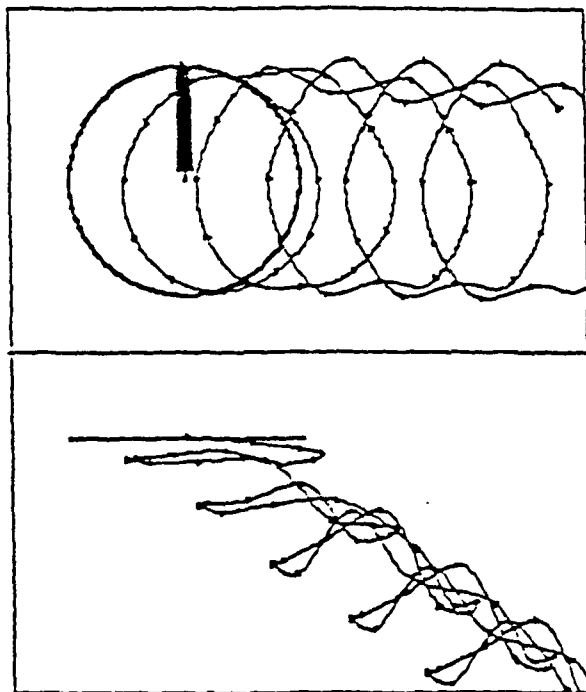


Figure 14. Free wake solution for a single bladed rotor at low forward speed (advance ratio = 0.10). Solution computed using an updated linearized far field with the exact ANM near-field correction.

Conclusions

A new approach to vortex filament velocity calculations has been developed based on the method of Analytical/Numerical Matching (ANM). This method combines the efficiency and far-field accuracy of vortex

particles, which are the simple discretization of the Biot-Savart integral, with an analytical correction that provides high near-field accuracy without the need to use high element densities to meet the near-field accuracy requirements. The ANM method provides a natural and mathematically correct distinction between far-field and near-field regions in a vortex wake, which is implemented in a manner analogous to the method of matched asymptotic expansions. Furthermore, the method is sufficiently simple to allow analytical linearization of the velocity expressions. As a result, all or part of the velocity expression can be linearized, allowing several options for additional gains in efficiency.

The results show accuracy comparable to that of curved vortex elements at a fraction of the cost: the current efficiency gains of a factor of 5 for the fully nonlinear solution are expected to double (a net of an order of magnitude) with refinement to a more efficient code. The linearized velocity expressions can be evaluated at 1/20th the cost of curved elements on a scalar computer, and vectorizing computers should provide further improvements. The ANM near field correction was shown to remove the discretization error associated with a low resolution vortex particle solution while accurately predicting the large gradient near field velocities. It was also shown that some care must be used in selecting the fat core parameter which is used to smooth the particle solution and to match the particle and analytical solutions. The ANM methodology has been incorporated into a helicopter free wake code, where it has compared well with the more computationally expensive curved vortex solutions.

Acknowledgements

This research was sponsored by a NASA Graduate Student Researchers Program Fellowship, Grant No. NGT-50169 under the Rotorcraft Aeromechanics Branch at the NASA Ames Research Center, and U. S. Army Research Office Grant No. DAAL03-88-K-0062. The authors would like to thank the NASA technical monitors William R. Warmbrodt and Fort F. Felker, and the ARO technical monitor Thomas Doligalski.

References

1. Burt, D. B., Teske, M. E., & Quackenbush, T. "A New Methodology for Free Wake Analysis Using Curved Vortex Elements," NASA CR-3988, 1987.
2. Couet, B., Buneman, O., & Leonard, A., "Simulation of Three-Dimensional Flows with a Vortex-In-Cell method," J. Comp. Phys., Vol. 39, 1981, pp. 305-328.
3. Leonard, A., "Vortex Methods for Flow Simulation," J. Comp. Phys., Vol. 37, 1980, pp. 289-335.

4. Baker, G. R., "The Cloud-In-Cell Technique Applied to the Roll Up of Vortex Sheets," *J. Comp. Phys.*, Vol. 31, 1979, pp. 76-95.
5. Bliss, D. B., Dadone, L., & Wachspress, D. A., "Rotor Wake Modeling for High Speed Applications," *Proceedings of the 45th Annual Forum of the American Helicopter Society*, May, 1987.
6. Rosenhead, L., "The Spread of Vorticity in the Wake Behind a Cylinder," *Proceedings of the Royal Society of London, Ser. A-127*, 1930, pp. 590-612.
7. Batchelor, G. K., "An Introduction to Fluid Dynamics," Cambridge University Press, Cambridge, England, 1967, pp. 509-511.
8. Bliss, D. B., Wachspress, D. A., & Quackenbush, T. R., "A New Approach to the Free Wake Problem for Hovering Rotors," *Proceedings of the 41st Annual Forum of the American Helicopter Society*, May 1985.
9. Bliss, D. B., Teske, M. E., & Quackenbush, T. R., "Free Wake Calculations Using Curved Vortex Elements," *Proceedings of the International Conference on Rotorcraft Basic Research*, sponsored by the Army Research Office and the American Helicopter Society, Feb. 1985.
10. Bliss, D. B., Quackenbush, R. T., & Bilanin, A. J., "A New Methodology for Helicopter Free Wake Analysis," paper A-83-39-75-000, presented at the 39th Annual Forum of the Am. Helicopter Soc., May 1983.
11. Hooper, W. E., "The Vibratory Loading of Helicopter Rotors," Paper No. 46, 9th European Rotorcraft Forum, Sept. 1983.
12. Abramowitz, M. & Stegun, I. A., "Handbook of Mathematical Functions with Formulas, Graphs, and Mathematical Tables," National Bureau of Standards Applied Mathematics Series 55, 10th Printing, Dec. 1972, pp. 591-592.
13. Bliss, D. B. & Miller, W. O., "Efficient Free Wake Calculations Using Analytical/Numerical Matching and Far-Field Linearization," *Proceedings of the 45th Annual Forum of the American Helicopter Society*, May 1989.

Efficient Free Wake Calculations Using Analytical/Numerical Matching and Far-Field Linearization

Donald B. Bliss* and Wayne O. Miller**

Duke University, Durham NC

ABSTRACT

A hybrid analytical and numerical method called Analytical/Numerical Matching (ANM) is used to calculate the velocity field of rotor wake vortex filaments. A simple discretization of the Biot-Savart law is used to obtain an efficient but low resolution numerical calculation of the velocity field. A fictitious large vortex core is introduced and the discretized velocity field is calculated accurately for a smooth large core filament. At points close to the filament, a local analytical correction based on the Biot-Savart law for a curved vortex filament is employed to remove the nearfield error and add the correct nearfield velocity contribution associated with the actual core size. Because this correction is computationally inexpensive, the overall approach is both very efficient and very accurate. The accuracy of the ANM method has been studied in detail for vortex rings. Free wake solutions are obtained much faster using the ANM method in comparison to other methods with comparable accuracy. Because ANM is functionally simple, it is possible to obtain derivatives of the velocity expressions in closed form using a symbolic manipulation program. By computing derivatives of the velocity field the free wake calculation has been linearized. The linearized form is computationally efficient since it avoids large numbers of repetitive Biot-Savart law calculations. Linearized free wake problems are solved by a time marching method and compared with full nonlinear results. A special mathematical approach to obtain solutions for linearized periodic wake motion by a method that does not involve time marching is also discussed. This approach finds periodic solutions directly by inversion of a large matrix.

Introduction

Free wake calculations, which allow the wake vorticity field to evolve in free motion, are the most accurate and physically correct approach to rotorcraft aerodynamics. From their inception, however, these calculations have been plagued by several difficulties, including the inadequacy of oversimplified physical models of the wake, excessive computer time, questionable numerical accuracy, and convergence problems. As a result, free wake analyses still have not achieved their potential impact in rotorcraft engineering. However, there has been considerable progress in recent years. It is now apparent that a full-span computational treatment of the vortex wake is necessary for many flight conditions^{1,2}, as opposed to earlier codes which relied on tip vortex models and, at most, a relatively casual treatment of the inboard wake. Therefore, for future free wake analyses to be accurate, they must deal computationally with the motion of much larger vorticity fields than in the past. The high resolution analysis of multi-blade, full-span free wakes of extended length is a significant challenge even for modern computational capabilities.

* Associate Professor, Mechanical Engineering.

** Graduate Student, Mechanical Engineering.

Presented at the 45th Annual Forum of the American Helicopter Society, Boston, MA, May 1989.

Thus the problems of efficiency, accuracy and convergence remain. These problems must be judged in the context of the demands to be placed on codes with realistic predictive capabilities. Along with a converged free wake calculation, such a code must predict blade dynamic motions and match trim conditions for lift, thrust, and side force. In the current iterative approach to this multi-faceted problem, it is actually necessary to converge the free wake part of the solution repeatedly just to gain results for a single trim condition. It is worth noting that this iterative approach is both inefficient and physically incorrect.

In spite of the availability of ever more powerful computers³, there is a need to reduce the computer time required for free wake calculations by several orders of magnitude. The free wake formulation must also be rendered more compatible with the calculation methods for blade dynamics and aerodynamics, so that these aspects of the problem can be solved simultaneously rather than iteratively.

This paper describes a new approach to free wake analysis intended to address these problems of efficiency and compatibility. This new approach differs from previous methods in the following respects: it uses an efficient new method for computing the wake velocity field; it distinguishes

The main features of this research, as they appear in the paper, are as follows. A hybrid analytical and numerical method called Analytical/Numerical Matching (ANM) is used to calculate the velocity field of rotor wake vortex filaments. This approach is found to give accuracy comparable to the best available curved element methods with greatly reduced computer time. Sample calculations are presented for vortex rings and for rotor wakes. Because ANM is functionally simple, it is possible to linearize all or part of the free wake calculation, and thereby avoid large numbers of repetitive Biot-Savart law calculations. The time marching solution procedure for a linearized free wake is described and sample

Velocity Calculations Using Analytical/Numerical Matching

Analytical/Numerical Matching (ANM) is a hybrid analytical and numerical method used to calculate the velocity field of the wake vortex filaments. This new procedure obtains an accurate velocity field by combining a low resolution numerical solution and a high resolution analytical

First a low resolution numerical calculation of the velocity field is achieved by summing over a field of discrete values of the Biot-Savart integrand, which gives the simplest possible approximation to the Biot-Savart integral. This approach is similar in some respects to the use of "vortex particles" or "vortons", but with an important difference. The vortex particle formula is altered mathematically to produce a smoothing effect similar to a very large (fat) vortex core. The expression for the velocity induced at a point by a vortex filament is as follows:

$$\vec{v} = -\frac{\Gamma}{4\pi} \int_C \frac{\vec{r}_v \times d\vec{s}}{r_v^3} = \sum_{i=1}^N \frac{\vec{r}_v \times \Delta \vec{l}_i}{[r_{vi}^2 + r_c^2]^{3/2}}$$

Here r_{ij} is the distance from the i th vortex element to the point of evaluation, and Δl_j is vector distance between collocation points (an effective element length). This equation shows how the Biot-Savart integral is discretized and how the vortex core effect is introduced through the inclusion of a core size length scale r_c . For the case of a straight vortex filament the above equation gives a two-dimensional swirl velocity distribution of the form

$$v = - \frac{\Gamma}{2\pi} \frac{r}{r^2 + r_c^2}$$

For $r \ll r_c$ the swirl velocity behaves like solid body rotation, and for $r \gg r_c$ the swirl velocity behaves like a potential flow point vortex. The swirl velocity reaches a maximum at $r = r_c$.

Using these fat core vortex particles, it can be shown that when the core size length scale r_c exceeds the spacing between particles, the discrete numerical treatment accurately simulates a continuous vortex filament with the same large core properties. This fact, represented schematically in Figure 1, allows for the very efficient calculation of a smoothed (fat core) flow field by the simplest possible means. However, if taken alone this calculation gives an accurate answer to the wrong problem because the core is too large.

The solution can then be corrected analytically to obtain the right answer. The local solution for the velocity field near a curved arc filament can be obtained in closed form. At the point on the filament nearest the point of evaluation (and only at this point), two overlaid curved arc solutions are added the numerical result. The overlaid analytical solution consist of an arc with the correct core size and correct sign circulation and a fat core arc with the opposite sign circulation. These analytical arc solutions are based on the velocity field around a vortex ring, with the elliptic integral functions appearing in this expression represented by polynomial curve fits.

Referring again to Figure 1, for the portion of the filament nearest the point of evaluation, the opposite sign fat core arc cancels the fat core numerical solution leaving the contribution of the arc with the correct core size. For the portion of the filament away from the point of evaluation, and beyond the edge of the fat core, the two analytical arc solutions cancel each other leaving the numerical solution, which is accurate at points beyond the fat core. The sum of the fat core numerical solution, the actual core arc, and the opposite sign fat core arc form a uniformly valid composite solution (see Figure 1). The procedure to construct the solution can be stated concisely as:

$$\begin{aligned} \text{Composite Soln} &= \text{Fat Core Numerical Soln} \\ &+ \text{Actual Core Analytical Soln} \\ &- \text{Fat Core Analytical Soln} \end{aligned}$$

This approach corresponds to the mathematical procedure called Matched Asymptotic Expansions (MAE) in which a composite solution is constructed by matching inner and outer solutions. In the present case, the fat core numerical solution is analogous to the outer solution, the analytical arc with the correct core is the inner solution, and the opposite sign fat core analytical arc is analogous to the inner limit of the outer solution and the outer limit of the inner solution. The MAE composite solution is constructed in exactly the manner described above, namely

$$\begin{aligned} \text{Composite Soln} &= \text{Outer Soln} \\ &+ \text{Inner Soln} \\ &- \text{InnerOuter (or OuterInner)} \end{aligned}$$

As in matched asymptotic expansions, the ANM method requires there to be an overlap region between the farfield numerical solution and the nearfield analytical solution. This overlap is achieved by judicious choice of the vortex particle core size in relation to the particle spacing. The core size must be sufficiently large to have the numerical calculation of the nearfield velocity be smooth along the vortex filament: as if the filament were continuous rather than discretized. In practice, values of r_c greater than or equal to half the filament spacing satisfy this smoothness criterion to very good accuracy (errors not greater than a few percent anywhere within the vortex core). On the other hand, if the core size is too large, the proper cancellation of terms in the composite solution may not be achieved. In the region where the shape of the local analytical arc and the actual filament become disparate, all the contributors to the composite solution must be sufficiently far outside the core that each appears as a potential flow. Because the core effect decays relatively slowly (algebraically), it is best to keep the core as small as possible and still satisfy the smoothness criterion. In practice, this means that values of r_c should be between one-half and one times the element spacing to achieve the best overall accuracy.

A serious criticism of current free wake methods is that an enormous amount of computer time is spent calculating the effect of vortex elements relatively far from the point of evaluation. Past efforts to circumvent this problem have been of an approximate nature, typically not updating certain portions of the wake velocity field in the numerical routine as the wake evolves. The distinction between nearfield and far-field regions is illustrated in Figure 2. The farfield induces a smooth, slowly varying velocity field on the point of evaluation, whereas the nearfield is associated with strong, rapidly varying interactions. The current approach allows a formal distinction between farfield and nearfield effects. By the appropriate choice of scales, the numerical fat core free wake plus the (opposite sign) analytical fat core arc constitute the effective far field solution, making it unnecessary to define a special proximity criteria to determine which portions of the wake may be simplified for efficient far-field treatment. The analytical actual core arc solution, which is the remaining part of the overall solution, is entirely responsible for the strong, typically nonlinear, nearfield effects. The fact that the nearfield/farfield distinction arises naturally in the new method allows for the implementation of a formally correct procedure for more efficient wake calculations, as described later.

The relationship between this method and other vortex elements should be discussed. Previous work has dealt primarily with elements that provide a geometric fit to the vortex filament. These elements correspond to a closed form Biot-Savart integration of a segment of vortex filament. The overall filament velocity field is then determined by numerically summing the contributions from these individual segments. Straight-line elements have been frequently used to provide a piecewise linear fit to curved wake filaments. Basic Curved Vortex Elements (BCVE's)⁴⁻⁷ are based on a parabolic fit and this curved element provides inherently better accuracy. Although BCVE's are more computationally expensive on a per element basis, their fitting accuracy is sufficiently superior that many fewer elements can be used, leading to a net improvement in computational efficiency. The so-called vortex particle method, which is merely a simple discretization of the Biot-Savart integral, is the most computationally efficient approach by virtue of its functional simplicity, but it does not represent a geometric approximation of the vortex filament. The present method, which is based in part on the vortex particle approach, first removes the severe nearfield discretization errors of the vortex particles by artificially smearing the singularity. This smearing is achieved by introducing the core parameter r_c into

the denominator of the Biot-Savart integrand. When properly done with overlapping cores, the result effectively bridges the gap between particles, providing the equivalent of a geometric fit between the filament collocation points. The nearfield analytical correction is then applied to achieve the correct core size. This correction is applied only at the point on the filament where the distance to the point of evaluation is a minimum, and then only if this point is close enough to the filament for the correction to make a difference. Thus, the nearfield correction is applied only rarely. The present method successfully retains the speed and simplicity of vortex particles, while properly modeling filament curvature effects and achieving the high nearfield accuracy associated with BCVE's.

An added advantage of the ANM method, to be discussed later, is that the formulation is sufficiently simple analytically to allow linearization of the velocity expressions in closed form. As a result, all or part of the wake velocity calculation can be linearized, allowing for additional simplifications and new solution strategies for free wake analysis.

Finally, it should be mentioned that the method of Analytical/Numerical Matching (ANM), developed at Duke University to analyze vortex filament dynamics⁸, has recently been applied to other problems in aerodynamics. These applications include modeling vortices in the nearfield of a paneled surface for interactional aerodynamics⁹, and modeling the high resolution flow field through a tail rotor disk¹⁰. In fact, ANM appears to have general applicability to a number of problems involving singularity distributions, and is not limited to problems involving vortex filaments.

Accuracy of the ANM method

The numerical verification of the ANM approach was based on calculating the velocities induced by a closed circular vortex ring. The ring geometry was chosen because a closed-form analytical result for the induced velocity is known, and previous ring studies^{4,6,7} using the BCVE and straight-line elements were available for comparison. The ring geometry used is presented in Figure 3.

A primary advantage of the ANM method over simple vortex particles is the smoothing of the particle discretization error which is noticeable at distances less than the particle spacing. Figure 4 illustrates this smoothing in the swirl velocity component of a ring with 30-degree particle spacing. The vortex particle solution is seen to be strongly affected by proximity to individual particles (azimuthal location) at distances from the ring of less than one particle spacing. In comparison, the ANM solution is essentially constant at all azimuthal locations, and is accurate at all distances from the ring. Similar results are obtained for the other two velocity components. It is possible to smooth out the discrete particle solution just by the use of a core size larger than the particle spacing, but large cores are in general non-physical and will underestimate the strong near-field induced velocities. The ANM method provides good accuracy using any core size.

The ANM solution is compared to vortex particles, straight line elements and BCVE elements in Figure 5, which examines the vertical velocity predictions directly above a ring. The ordinate is the normalized velocity error and the abscissa is the ratio of the distance above the ring to the element length. The ANM solution is seen to be very accurate as the ring is approached, surpassing even the BCVE solution close in. At a distance of one element spacing, the ANM solution is an order of magnitude more accurate than the vortex particles, and two orders of magnitude better than the straight line elements. In a practical sense, at distances larger than one element spacing all methods are sufficiently accurate, reinforcing the observation that the ANM method is

essentially a near field correction procedure used to capture the strong nonlinear nearfield velocities. As the current ANM implementation is based on a circular arc geometry, this high accuracy is to be expected, although general curved filaments are also accurately modeled as suggested in the rotor simulations discussed later. As with any curve fitting elements, the ANM solution deteriorates as the resolution gets too low (e.g. arcs greater than about 60 degrees between collocation points). Resolution is a separate issue that must be addressed when defining the wake model.

The ANM approach was found to be computationally efficient as well as accurate. For N vortex elements, the CPU time for a complete wake velocity computation may be given by a quadratic in N as $T = A + BN + CN^2$, which for large N is dominated by the squared term. Figure 6 compares the quadratic coefficient C normalized to the BCVE coefficient for several element types. The coefficient C is of interest because large free-wake calculations are dominated by this N^2 term, which corresponds physically to the effect of every vortex element on every other element. The ANM method is seen to be more than three times faster than the BCVE element, while the vortex particles alone are five times faster than the BCVE. Recall that the ANM corrections are applied selectively to the nearfield interactions, while particles are used alone for most of the wake, resulting in an overall efficiency gain between 3 and 5 times that of the BCVE. There is reason to believe that an additional factor of two can be achieved by reformulating the elements using a parabolic fit rather than a circular fit, and by avoiding the local coordinate transformations used in the present implementation, resulting in a speed up of 6 to 10 over the BCVE. Figure 6 also shows the time necessary to compute the analytical linearization of the ANM velocities, which is discussed below.

Linearized Velocity Analysis

One justification for the development of the ANM method was that the near field of a vortex filament is characterized by a strong, rapidly varying velocity field which cannot be accurately described by vortex particles alone. By the same argument, the far field is characterized by a relatively weak and slowly varying velocity field, and these properties make the far field a candidate for linearization. Specifically, the velocities induced by the far field are spatially linearized about some initial configuration using a truncated Taylor series in the wake position variables. As the wake evolves in time, the farfield velocities are approximated by evaluating the resulting linear expression, rather than recomputing the exact particle velocities from the Biot-Savart law. Note that for traditional time-marching integration, this does not involve inverting the coefficient matrix, but only a matrix-vector multiplication. The linearized wake is re-used until the wake has evolved to the point where it is no longer accurate, at which time the wake is relinearized. Helicopters at moderate to high advance ratios have wakes that evolve relatively little, so that one linearization may suffice for an entire wake convergence calculation.

The linearized free-wake velocity problem takes the form of a large linear system (far field) with locally embedded nonlinearities (near field). Consistent with the matched asymptotic expansions approach of the ANM correction, the far field encompasses all of the vortex particles since their far cores remove the strong nearfield behavior. Furthermore, the fat and thin core components of the nearfield ANM corrections may each be linearized. The highest accuracy results from computing the ANM corrections exactly at each time step, while the maximum efficiency is found by linearizing both the particles and the ANM correction, resulting in a complete linear description of the wake

velocities. Between these extremes is the option of a linearized far field and a nonlinear near field. As indicated in Figure 6, the time to compute the complete linearization is 1.4 times that of a BCVE velocity calculation. The completely linearized velocity expression also has the advantage of placing the wake velocities in a form functionally similar to the blade dynamics problem, allowing the opportunity to solve these two aspects of the overall problem simultaneously in future work.

The use of vortex particles facilitated the analytical linearization of the wake velocities due to their simple functional form. Linearization of the ANM analytical nearfield correction was also possible, but with more effort due to the presence of elliptic integrals in their expressions. It is interesting to note that the closed-form derivation of the Taylor coefficients in the linearization were performed using SMP, a symbolic manipulation computer program similar to MACSYMA and Mathematica. The velocity expressions are functions of 12 scalar variables for each element, and the derivative calculations are quite lengthy. The use of SMP greatly reduced the chance of human error in these differentiations. The program was also used to translate the resulting symbolic representations directly into FORTRAN code. Subsequent code verification proved the derivative expressions to be correct.

Sample Free-Wake Calculations

The ANM and linearized velocity methods were incorporated into a rotor free-wake analysis program, adding to an existing BCVE analysis capability, to provide a practical testing situation. The program allows for multiple rotor blades with tip and root filaments. The free-wake is not abruptly truncated in space, but uses an analytical correction^{4,6} to extend the wake to infinity, which is physically consistent with Helmholtz' vorticity theorems. Two flight conditions are presented here: a two-bladed rotor at moderately high speed (advance ratio = 0.3) using 15 elements per turn of free wake, and a single-bladed rotor at low speed (advance ratio = 0.1) using 12 elements per turn of free wake. Both cases use 20-foot rotor blades at an angular velocity of 30 radians/second and a total thrust coefficient of 0.004. The blade disks have a forward tilt of 10 degrees, and only tip filaments were used. In both cases the results are presented as three orthographic projections of the wake (top, side, front) together with plots of the predicted velocities induced on the advancing blade. Note that the advancing blades have a Blade-Vortex Interaction (BVI) at roughly 80% of the span. Both cases use three turns of free-wake, and an additional two turns of the (infinite) far-wake extension are shown in the figures.

High-Speed Results

The wake at 0.3 advance ratio consists of two tip filaments generated by two blades. At this moderately high speed, the wake evolves relatively little from the idealized helical shape as the large filament separations reduce the strength and occurrence of near-field encounters. The ANM and BCVE solutions are shown in Figures 7 and 8 respectively, and are seen to be nearly identical. Both captured the downstream wake evolution and the advancing side roll-up. The velocities predicted on the blade differ slightly, due primarily to the different analytical treatments of the vortex core used by the two approaches (the BCVE method uses a solid-body rotation core, and the ANM method uses a core of the type described earlier).

Figure 9 presents the solution for a wake that was completely linearized at the outset about a skewed helix initial shape. The linearized wake converged to the configuration shown without further updates of the linearization. The

advancing side roll-up of the wake was not accurately captured, but is qualitatively correct. For this rotor loading ($C_T = 0.004$), a single linearization was adequate to locate a converged solution at this advance ratio and higher. At lower advance ratios, the linearizations needed to be updated or augmented with ANM nearfield corrections to reach an accurate converged configuration. Figure 10 presents the results for a fully linearized wake, but with an intermediate update of the linearization. The linearization is updated when the wake configuration evolves a specified distance from the linearization configuration, which provides a dynamic scheme for controlling the overall solution accuracy. The blade velocities are again predicted with good accuracy, and the advancing side roll-up is captured by the solution.

Low-Speed Results

The low-speed wake is generated by a single tip vortex filament. Because the loading is assumed to be the same as that for the two-blade high-speed case, the single filament has twice the strength of those at the higher advance ratio. This and the fact that a low speed wake is characterized by frequent near-field filament encounters results in a complex and convoluted wake structure. The low-speed case is thus a more demanding test of the ANM and linearized methodologies than the high-speed case. Figures 11 and 12 present the ANM and BCVE cases for comparison. The predicted wake structures near the blade disks are identical, but there is again some disagreement in the predicted peak BVI blade velocities which is attributable to the different analytical core treatments of the two methods. The retreating side roll up is essentially the same for both methods, but the stronger advancing side roll up differs somewhat in structure: the BCVE solution predicts a more pronounced horizontal rollup waveform as can be seen by comparing the top views in the two figures. However, the ANM solution predicts a stronger vertical rollup waveform which is more difficult to discern. The two linearized ANM cases discussed below each take one of these different forms as well, which indicates that the reason is not the unique difference between the analysis methods. It is presently suspected that these may represent two valid solutions to the inherently nonlinear wake evolution problem.

Figure 13 presents a completely linearized converged wake. The linearization was updated 6 times over a run of 11 revolutions to maintain validity as the wake evolved from the initial skewed helix, and was able to accurately match the solution reached by the ANM method given in Figure 11. However, the ANM solution required only 7 revolutions to converge and the BCVE solution 8 revolutions, indicating that the efficiency of the completely linearized wake solution suffers for strong low-speed wakes, as might be expected because these wakes undergo relatively large displacements as they evolve. Figure 14 presents a hybrid approach that used a linearized particle far-field with a nonlinear ANM nearfield. The far field was linearized twice over a run of 7 revolutions, and the wake converged to a configuration consistent with the BCVE solution (Fig. 12). The blade velocities predicted by both the linearized and hybrid solutions are essentially identical to the ANM results.

Alternative Solution Method

Finally, the linearized formulation of the free wake problem allows special solution strategies to be employed. Suppose the entire velocity field is linearized, which is a particularly good approximation in high speed flight. The linear form then allows periodic solutions to this problem to be found by direct mathematical means, without the use of time marching. This method involves recasting the problem in terms of constant age points on the filament (different from

the traditional Lagrangian points), linking motions between adjacent azimuthal locations, and applying periodicity conditions. The problem of obtaining a periodic solution is reduced to a single large matrix inversion, for which efficient methods are available. This approach is capable of finding periodic solutions directly in an unambiguous manner, since it does not depend on the convergence of a time marching process. In fact, such an approach does not require the temporal stability of the system, i.e. periodic solutions can be found even if the system is unstable. Nearfield nonlinearity can be included approximately by successive relaxations during which the near field is relinearized each time. Implementation of this scheme, and comparison with time marching results, will provide a new opportunity to study free wake convergence and stability in a fundamental way. It must be emphasized that this solution approach differs from that undertaken in all previous free wake analyses, although it bears a definite relationship to the influence coefficient relaxation method developed previously for wakes in hover ^{5,11-13}. It is potentially efficient because it avoids the large number of steps over many blade revolutions needed to achieve convective washout of the initial wake shape, as required by the traditional Lagrangian time marching approach. Furthermore, the method should be particularly efficient when successive points on a performance curve are to be obtained; since these points are nearly linearly close together, very few relaxation steps are required to move to adjacent points. The current status of this latest research is that the analysis has been completed and a few initial computer runs have been made to obtain preliminary results.

Conclusions

A new approach to free wake velocity calculations has been developed based on the method of Analytical/Numerical Matching (ANM). This method combines the efficiency of the simplest discretization of the Biot-Savart integral with an analytic correction to achieve high nearfield accuracy. The results show that accuracy comparable to that of curved elements is achieved at a fraction of the cost. The ANM method provides a natural and mathematically correct distinction between farfield and nearfield regions in a vortex wake, thereby providing an opportunity to simplify farfield effects in a formally correct manner. Furthermore, the method is sufficiently simple to allow analytical linearization of the velocity expressions. As a result, all or part of the free wake calculation can be linearized. Comparisons have been presented to show the effects of total linearization and of farfield linearization in comparison to the full nonlinear solution. Furthermore, the effects of occasionally updating the linearization have been explored. Computer time and accuracy comparisons of these various cases have been presented. The degree to which these simplifications can be utilized without sacrificing accuracy depends on the advance ratio, the number of blades and the wake strength. Generally, a greater degree of linearization can be implemented at higher advance ratio where convective effects are stronger and free wake adjustments are smaller. Finally, linearization allows the implementation of new solution strategies for free wake analysis. Some novel methods involving time marching solutions have been demonstrated in the paper. Furthermore, a method that involves looking directly for periodic solutions of linearized wakes without time marching is also under development.

Acknowledgement

This research was sponsored by a Research Grant from the U. S. Army Research Office and a Graduate Student Research Fellowship from NASA Ames.

References

1. Bliss, D. B., Dadone, L., and Wachspress, D. A., "Rotor Wake Modeling for High Speed Applications," Proc. of the 43rd Annual Forum of the American Helicopter Society, May 1987.
2. Egolf, T. A., "Helicopter Free Wake Prediction of Complex Wake Structures Under Blade Vortex Interaction Conditions" Proc. of the 44th Annual Forum of the American Helicopter Society, Washington, DC, June 1988.
3. Egolf, T. A. and Massar, J. P., "Helicopter Free Wake Implementation on Advanced Computer Architectures" Proceedings of the 2nd International Conference on Rotorcraft Basic Research, sponsored by the Univ. of Maryland and the AHS, College Park, MD, Feb. 16-18, 1988.
4. Bliss, D. B., Teske, M. E., and Quackenbush, T. R., "A New Methodology for Free Wake Analysis Using Curved Vortex Elements," NASA CR 3958, Dec. 1987.
5. Bliss, D. B., Wachspress, D. A., and Quackenbush, T. R., "A New Approach to the Free Wake Problem for Hovering Rotors," Proc. of the 41st Annual Forum of the American Helicopter Society, May 1985.
6. Bliss, D. B., Teske, M. E., and Quackenbush, T. R., "Free Wake Calculations Using Curved Vortex Elements," Proceedings of the International Conference on Rotorcraft Basic Research, sponsored by ARO and the Amer. Helicopter Soc., Research Triangle Pk., NC, Feb. 1985.
7. Bliss, D. B., Quackenbush, T.R. and Bilanin, A.J., "A New Methodology for Helicopter Free Wake Analyses," paper A-83-39-75-000, presented at the 39th Annual Forum of the American Helicopter Society, St. Louis, Missouri (May 9-11, 1983).
8. Bliss, D. B. and Miller, W. O., "Vortex Filament Calculations by Analytical/Numerical Matching with Comparison to Other Element Methods," presented at the AIAA 9th Computational Fluid Dynamics Conference, Buffalo, NY, June 14-16, 1989.
9. Quackenbush, T. R. and Bliss, D. B., "Free Wake Calculation of Rotor Flow Fields for Interactional Aerodynamics," Proc. of the 44th Annual Forum of the American Helicopter Society, Washington, DC, June 1988.
10. Quackenbush, T. R., Bliss, D. B., Mahajan, A. J., "High Resolution Flow Field Prediction for Tail Rotor Aeroacoustics," Proc. of the 45th Annual Forum of the American Helicopter Society, Boston, MA, May 1989.
11. Quackenbush, T. R., Bliss, D. B., Wachspress, D.A., "Free Wake Analysis of Hover Performance Using a New Influence Coefficient Method", NASA CR 4150, 1988.
12. Quackenbush, T. R., Bliss, D. B., Wachspress, D.A., "Computational Analysis of Hover Performance Using a New Free Wake Method," Proceedings of the 2nd International Conference on Rotorcraft Basic Research, sponsored by the Univ. of Maryland and the AHS, College Park, MD, Feb. 16-18, 1988. Submitted to the AIAA Journal.
13. Felker, F. F., Quackenbush, T. R., and Bliss, D. B., "Comparisons of Predicted and Measured Rotor Performance in Hover Using a New Free Wake Analysis," Proc. of the 44th Annual Forum of the American Helicopter Society, Washington, DC, June 1988. Submitted to the AHS Journal.

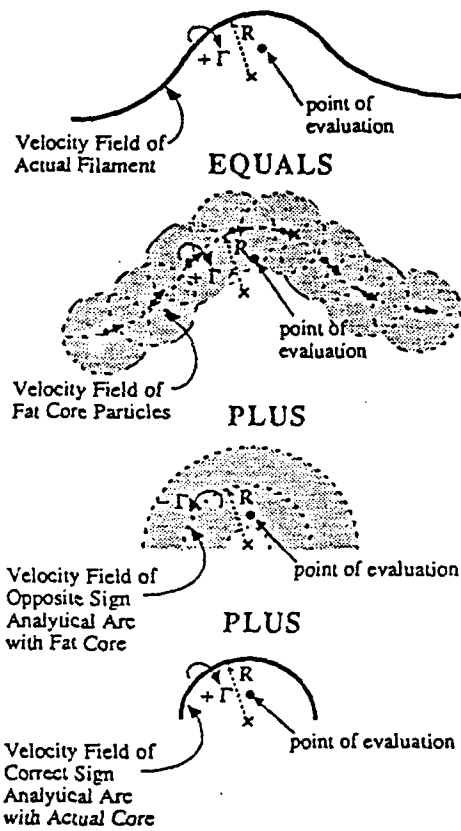
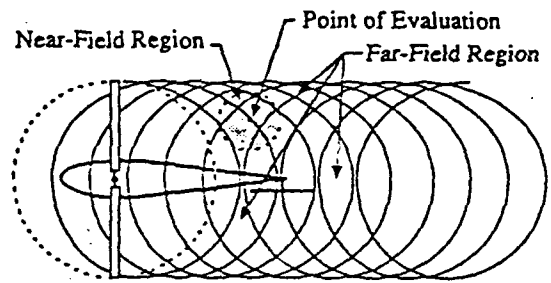


Figure 1. Construction of the ANM solution for the vortex filament velocity field by superposition of a low resolution numerical solution and local analytical solutions.



- Near-Field is in the immediate vicinity of the point of evaluation.
- Far-Field is the remainder of the wake.
- In the composite solution (Fig. 1), the far-field is composed of a fat core (low resolution) numerical free wake plus opposite sign fat core analytical arc. The near-field is represented by the actual core analytical arc.
- The smoothly varying far field effect can be linearized to avoid repeated Biot-Savart calculations for the vast majority of the wake.
- The rapidly varying near-field is expressible in terms of the relatively simple analytical arc solution.

Figure 2. Distinction between near-field and far-field free wake regions

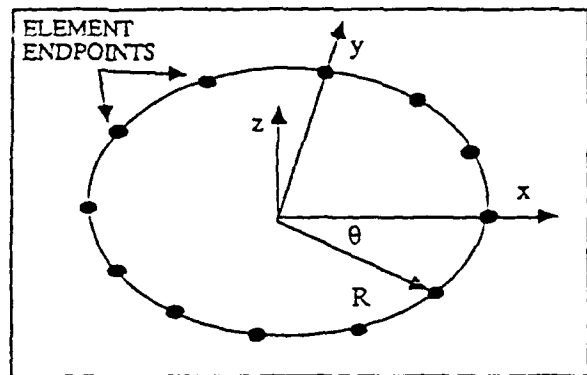


Figure 3. Vortex ring geometry used to verify numerically the ANM methodology.

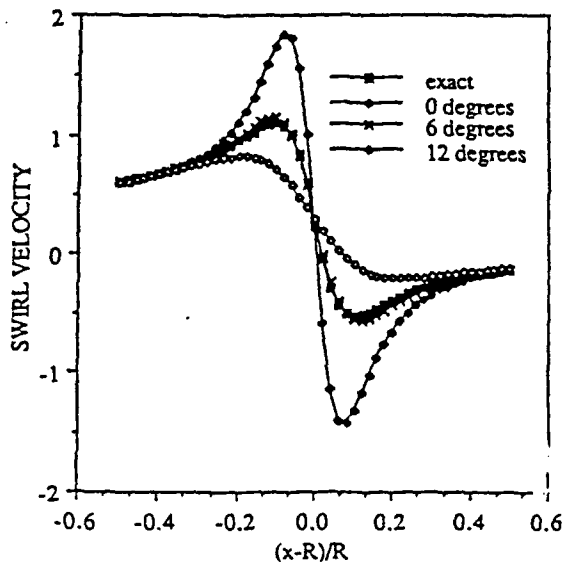


Figure 4a. Swirl velocity about a vortex ring modeled with 12 vortex particles. The velocity exhibits discretization error.

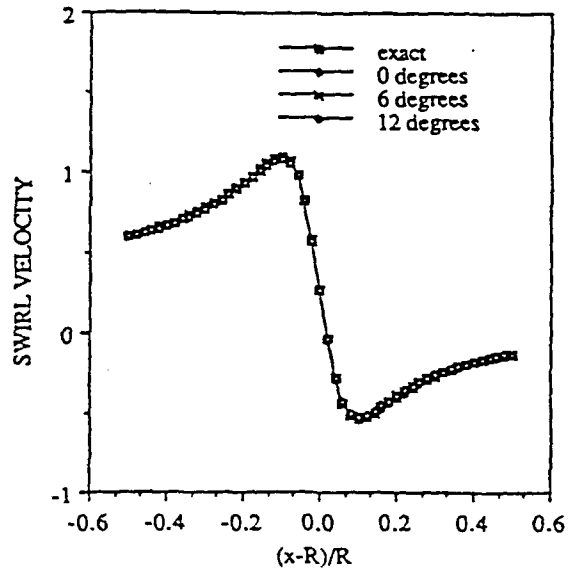


Figure 4b. Swirl velocity about a vortex ring using 12 vortex particles and the ANM correction. The discretization error is not evident.

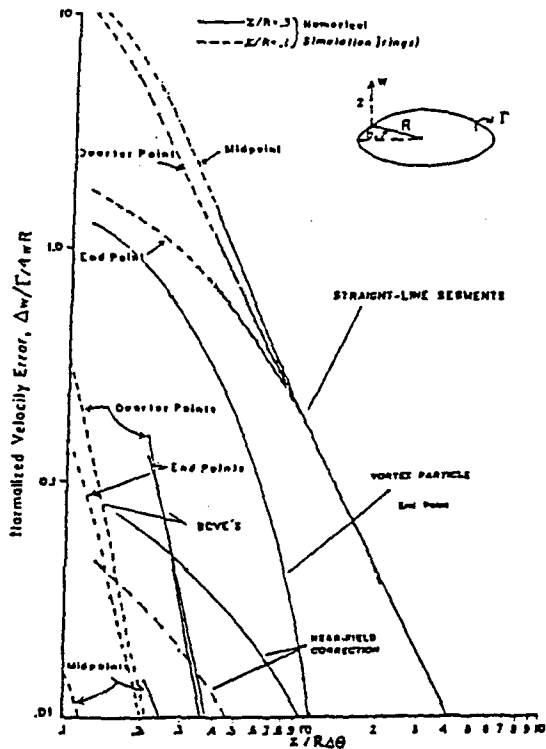


Figure 5. Errors in vertical velocity above a vortex ring as predicted by the ANM near-field correction, vortex particles, BCVE elements, and straight line elements.

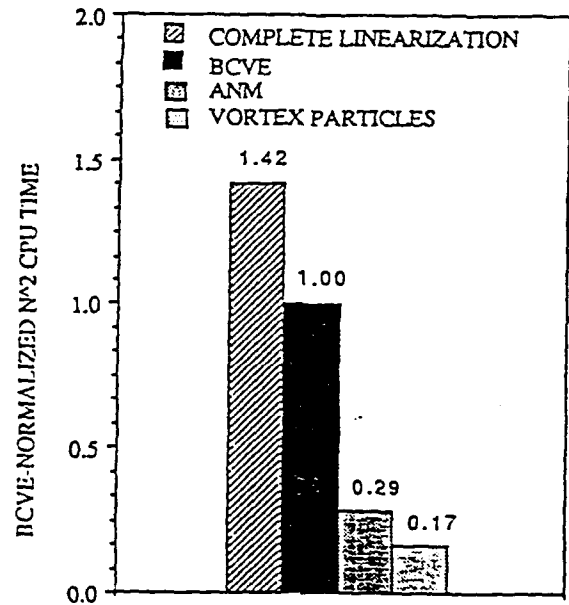


Figure 6. Computational efficiency for N^2 operations normalized to the BCVE element. (N = number of vortex elements).

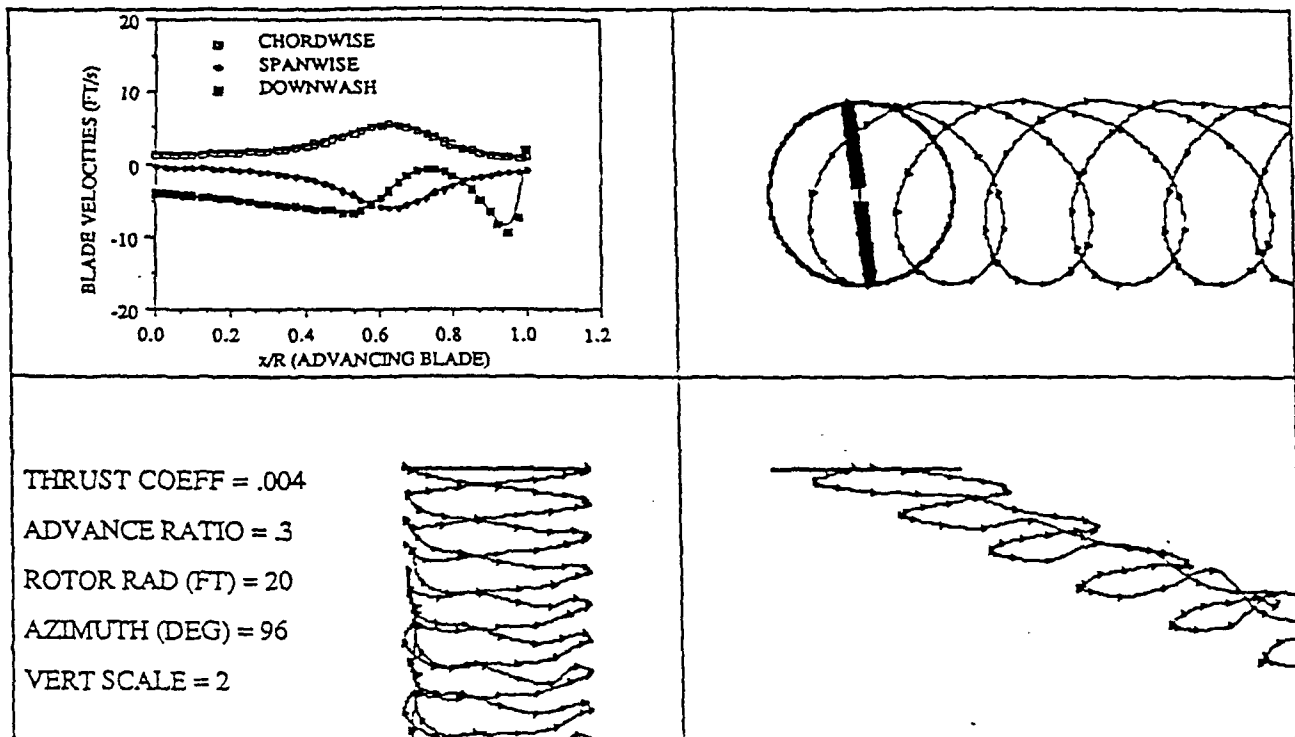


Figure 7. Wake solution and induced velocities on the advancing blade for an advance ratio of 0.3. Solution computed using the ANM near-field correction. Vertical scale expanded for clarity.

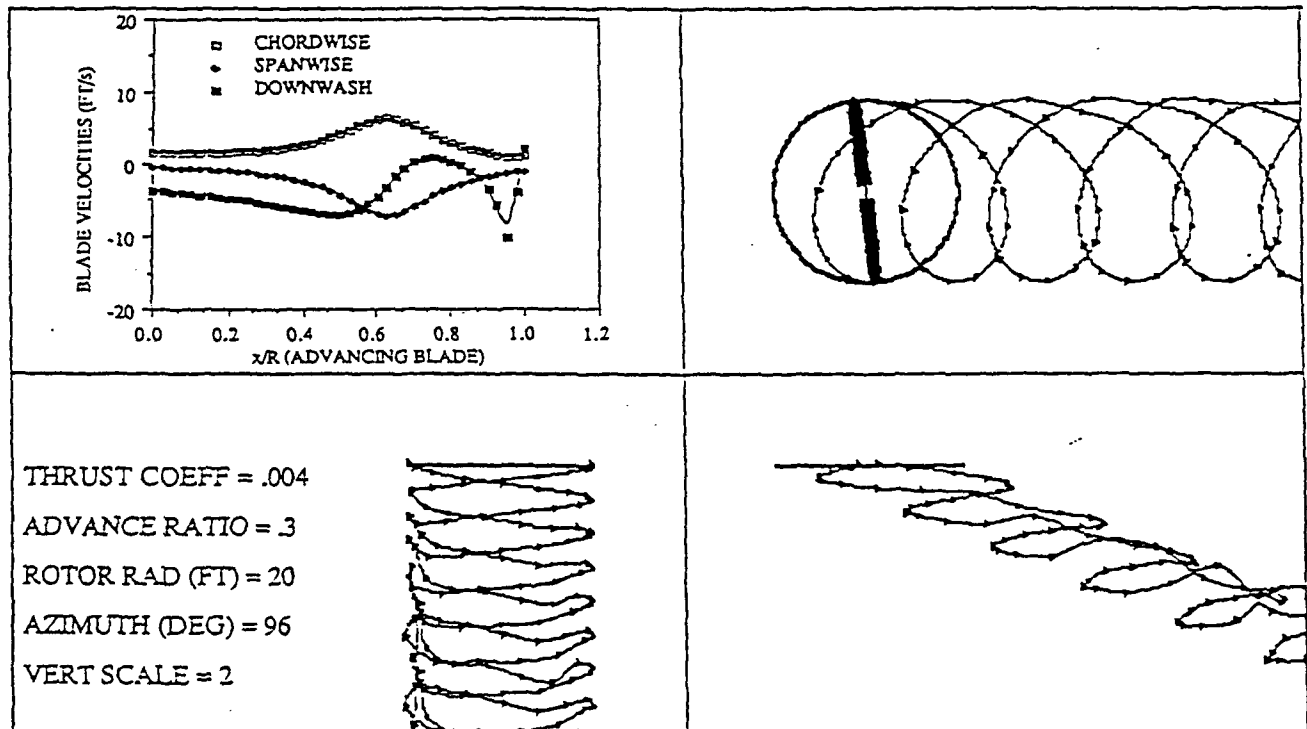


Figure 8. Wake solution and induced velocities on the advancing blade for an advance ratio of 0.3. Solution computed using the BCVE vortex elements. Vertical scale expanded for clarity.

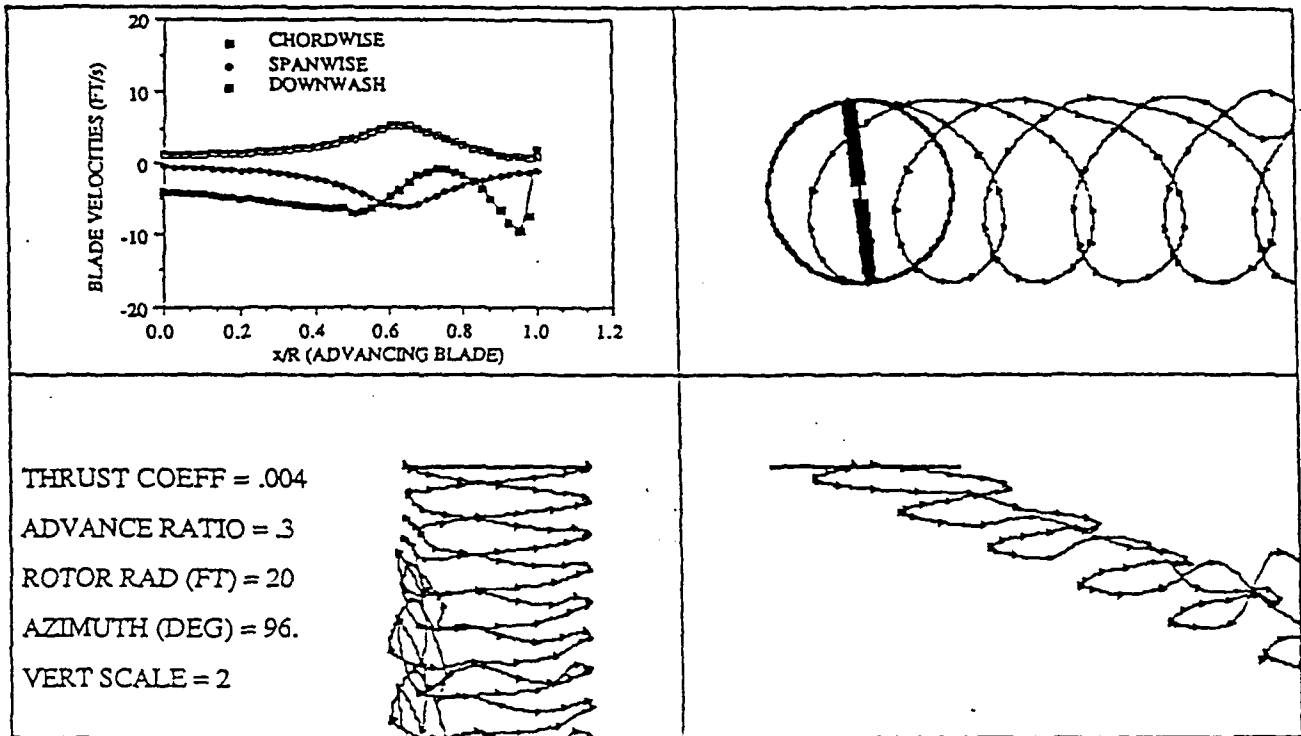


Figure 9. Wake solution and induced velocities on the advancing blade for an advance ratio of 0.3. Solution computed using the completely linearized wake analysis with only an initial linearization. Vertical scale expanded for clarity.

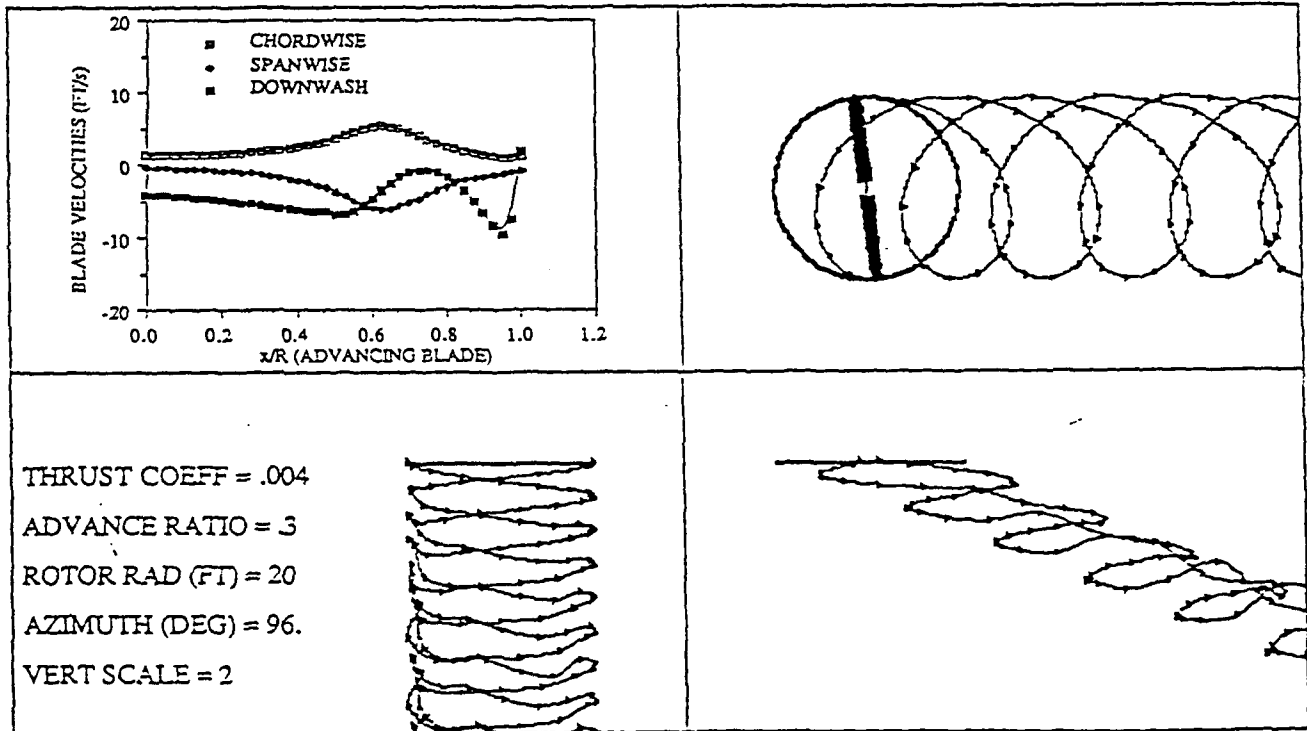


Figure 10. Wake solution and induced velocities on the advancing blade for an advance ratio of 0.3. Solution computed using the completely linearized wake analysis and an intermediate linearization update. Vertical scale expanded for clarity.

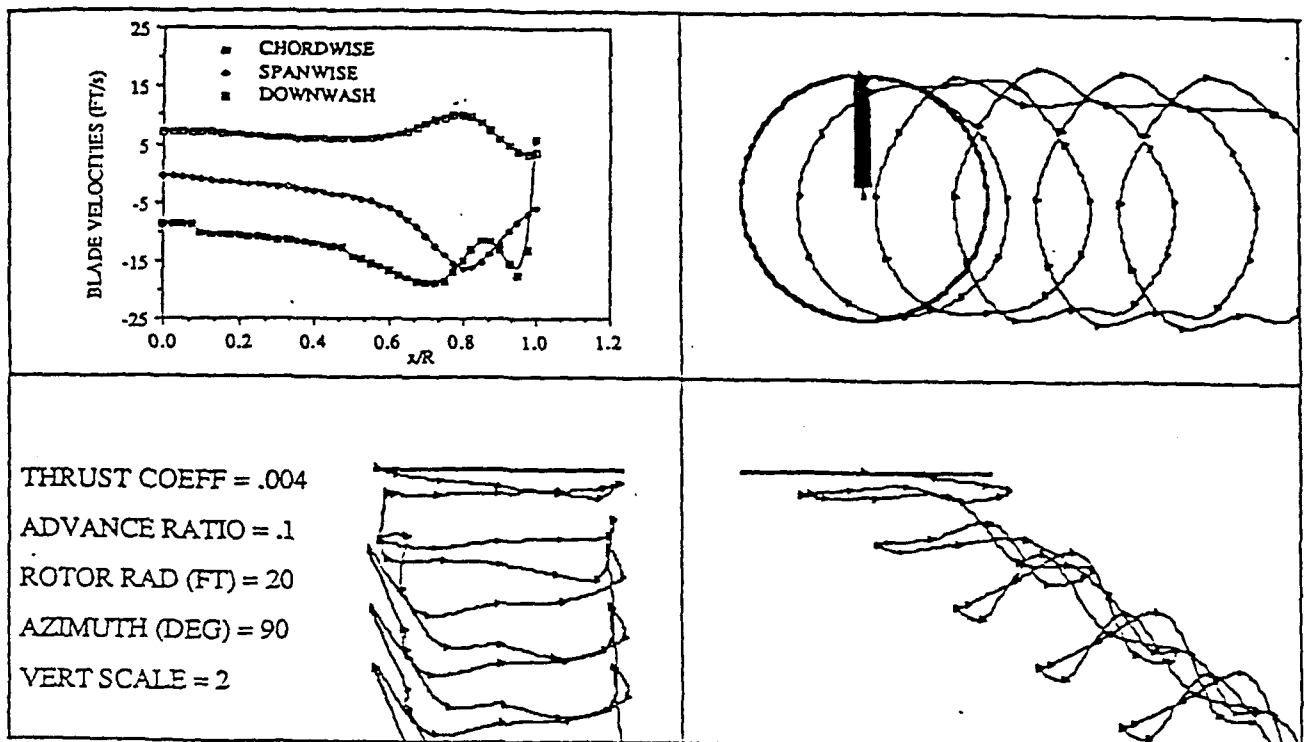


Figure 11. Wake solution and induced velocities on the blade for an advance ratio of 0.1. Solution computed using the ANM near-field correction. Vertical scale expanded for clarity.

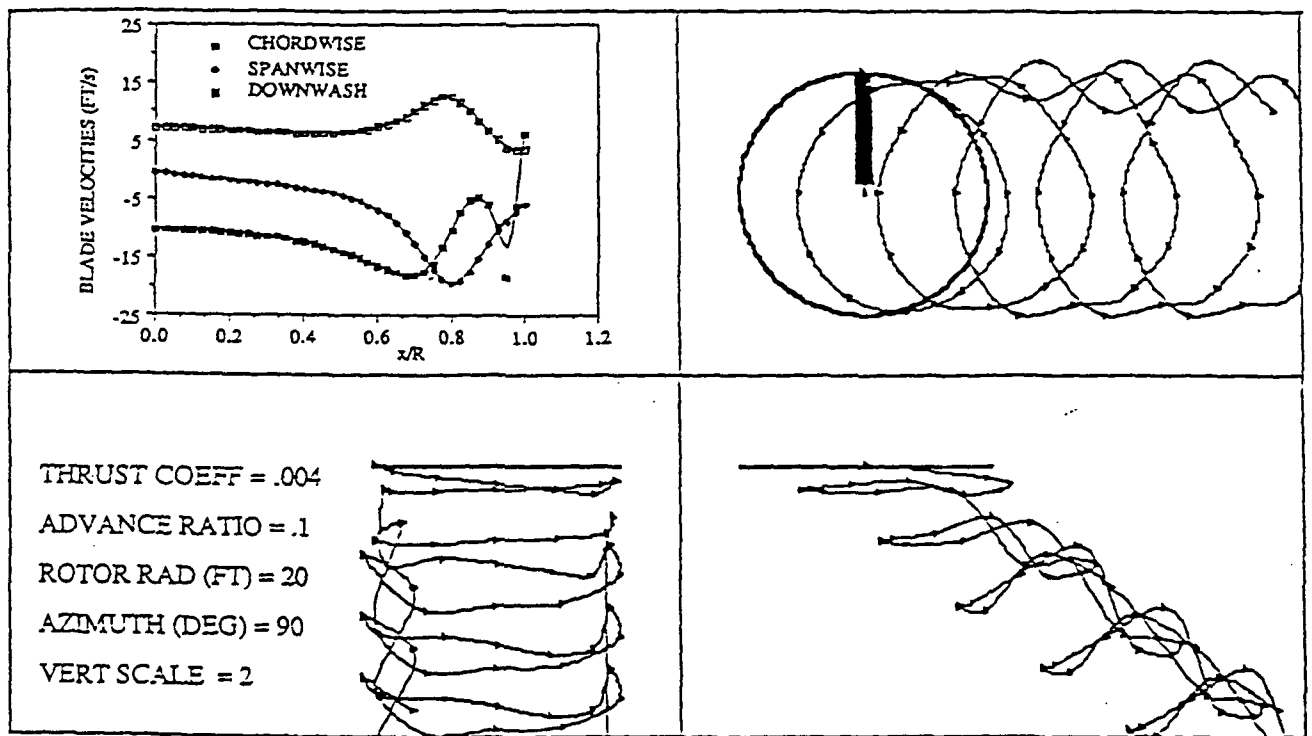


Figure 12. Wake solution and induced velocities on the blade for an advance ratio of 0.1. Solution computed using the BCVE vortex element. Vertical scale expanded for clarity.

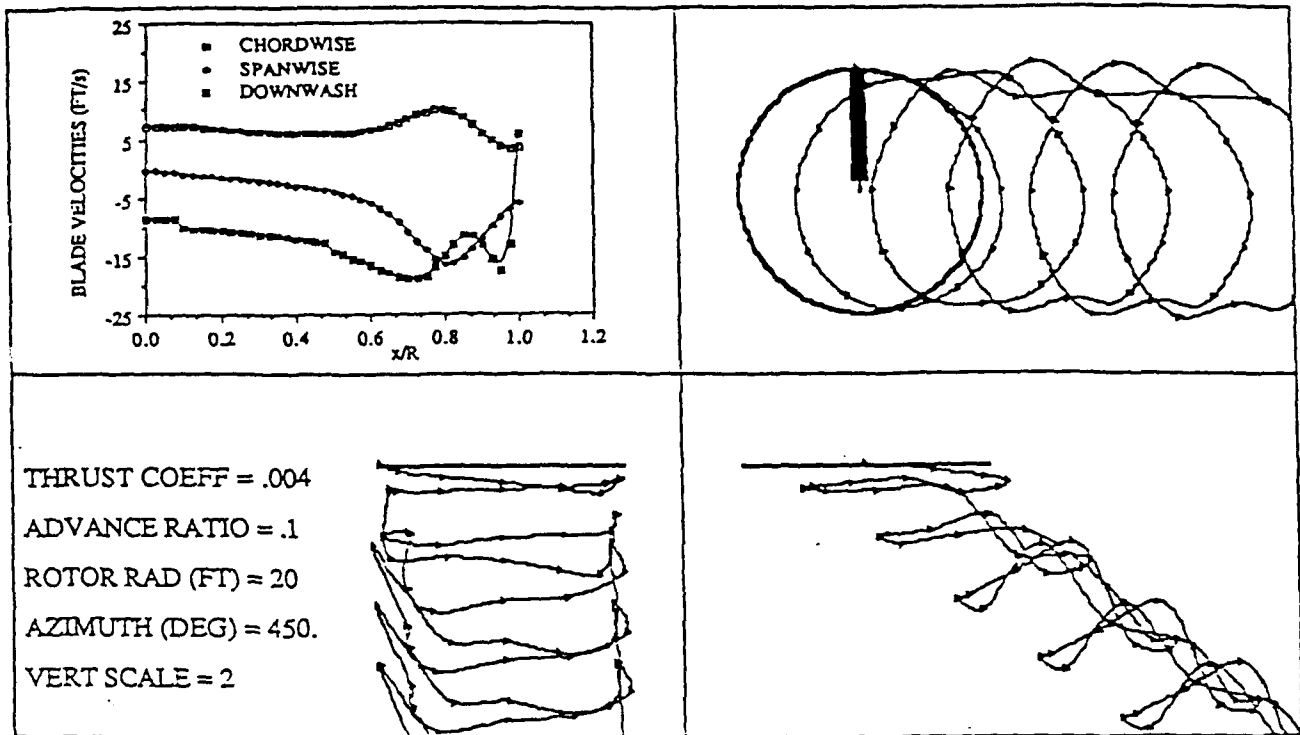


Figure 13. Wake solution and induced velocities on the blade for an advance ratio of 0.1. Solution computed using the completely linearized wake analysis and several intermediate linearization updates. Vertical scale expanded for clarity.

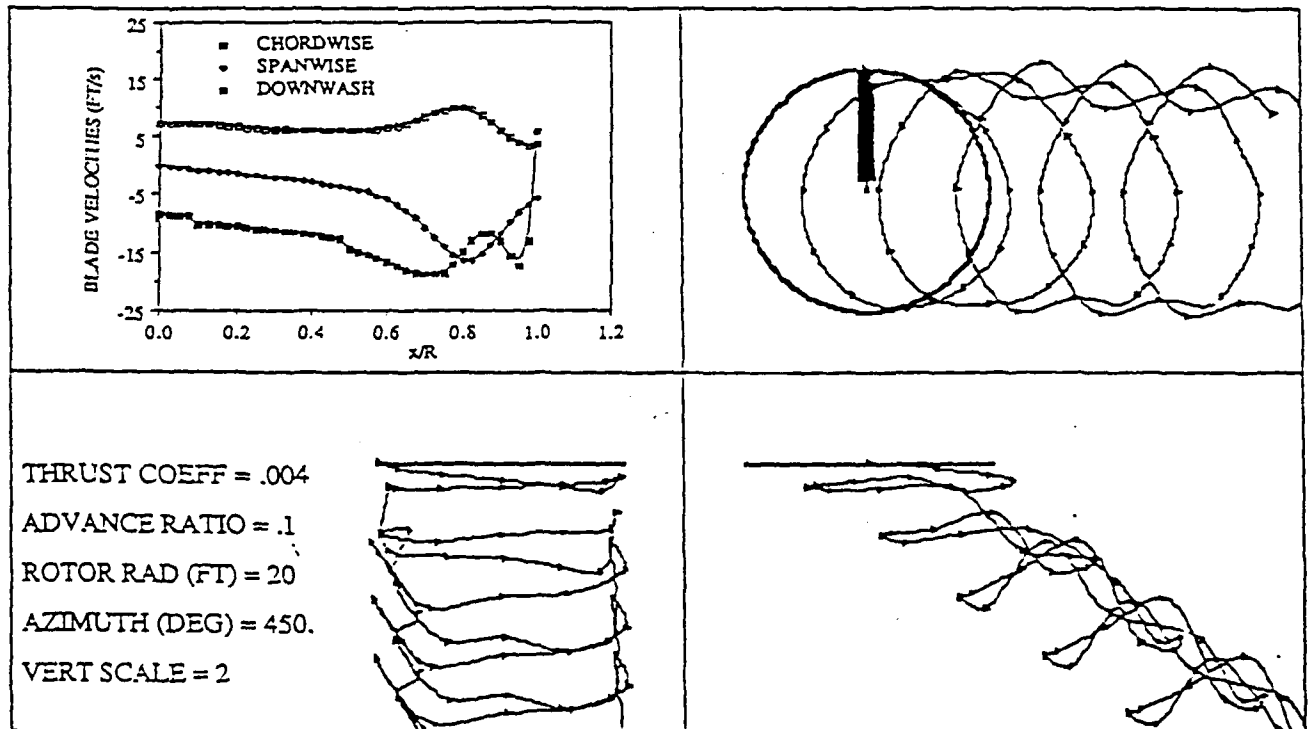


Figure 14. Wake solution and induced velocities on the blade for an advance ratio of 0.1. Solution computed using an updated linearized far wake with the ANM near-field correction. Vertical scale expanded for clarity.

Direct Periodic Solutions of Rotor Free Wake Calculations

By Inversion of a Linear Periodic System

Wayne O. Miller
Doctoral Candidate
Mechanical Engineering
Duke University
Durham, NC

Donald B. Bliss
Associate Professor
Mechanical Engineering
Duke University
Durham, NC

ABSTRACT

Periodic Inversion is a new approach for the calculation of rotor free wakes which guarantees periodically steady-state solutions, and provides the means to solve for wake dynamics at all advance ratios including low speed and hover. This is a unique capability since traditional time-marching approaches fail at low advance ratios. The method is based on enforcing periodic boundary conditions over $1/B$ of a rotor revolution, where B is the number of blades. This is accomplished by defining a new set of wake variables with periodic behavior, and writing the governing equations in a linear perturbation form. The problem is written as a large linear system which is inverted for the perturbative correction. Successive iterations involving relinearization are required to obtain the final solution to the nonlinear problem. The method allows converged solutions to be found without the use of artificial damping, even at low advance ratios and hover. Generation of performance curves is demonstrated as the flight parameters may be varied between iterations. The method is used to examine the low speed wake structure, which exhibits three unique forms depending on advance ratio: a helical structure from hover to some lower bound advance ratio, a roll-up structure above some higher bound advance ratio, and a rapid transition region between the two. Extensions of the method to allow coupling of the wake dynamics with panel methods and rotor dynamics are discussed, as are eigenvalue stability analysis and local element refinement.

INTRODUCTION

Free wake models, which allow the wake vorticity field to evolve in free motion, represent the most accurate and physically correct approach to rotorcraft aerodynamics. The simpler but less accurate approaches such as momentum theory and prescribed wakes have proven to be inadequate for predicting complicated aerodynamic blade loading [1,2,3]. From their inception, however, free wake calculations have been hampered by excessive computational effort and poor convergence behavior at low advance ratios and hover. Convergence in this context refers to the location of a wake structure which repeats every rotor revolution and is therefore steady state in a periodic sense. Indeed, because vortically induced velocity fields are inherently

nonlinear, the existence of unique and stable solutions remains an open question. Thus it is not surprising that the traditional time-marching approach to free wake dynamics encounters convergence difficulties.

Time-marching approaches begin with an assumed initial condition for the wake. As the integration proceeds, the errors in the initial wake are convected down and out of the free wake as it relaxes to a converged configuration. Exact convergence is never reached by time marching, but is approached asymptotically. In high-speed flight, the time-marching approach converges without difficulty as the free stream convection dominates the solution, thereby reducing the strength and frequency of the strongly nonlinear near-field vortex encounters. However, in low-speed flight the free stream effect is reduced, resulting in a dense field of wake vorticity and the dominance of the strong near-field interactions. At advance ratios below $\mu = 0.1$, the time-

Presented at the 46th Annual Forum of the American Helicopter Society, Washington, DC, May 1990

marching approach begins to exhibit poor convergence behavior. Initially, excessive time is needed to converge, but as the advance ratio is lowered the solutions tend to oscillate about some mean. Finally the solution diverges at a critical minimum advance ratio which depends on the specifics of the wake model. There is a limited amount of evidence to suggest that the wake dynamics may become chaotic at low advance ratios [4]. The limiting case of hover ($\mu = 0$) is unattainable for time marching codes unless artificial damping is introduced numerically. However, a special free wake method for hover has been developed that depends on the steady-state description of hover wakes in a rotating coordinate system [5]. At nonzero advance ratios this steady-state behavior is lost, so the method is not extensible to forward flight. There remains a range of flight conditions from hover to low speed which has previously been inaccessible for free wake models.

The method of Periodic Inversion presented here provides the means to study wake dynamics at low speed and hover using the accuracy of free-wake models. It also presents a method to generate performance curve data by varying flight parameters such as advance ratio μ , thrust coefficient C_t , and tip path plane angle TPP. The method is based on enforcing the periodic behavior of wakes in steady flight as a boundary condition. As such, a full period of wake is found at each iteration of the solution, compared to a single time step for time marching. Enforcing the periodic condition allows convergence of sensitive wake configurations without using artificial damping. In brief, the method involves describing the wake as a linear perturbation problem and solving for the perturbative corrections. The problem takes the form of a large linear system which describes the wake over a full period, and which is inverted for the perturbation correction vector. This description requires the linearization of the induced velocities given by the Biot-Savart law. This linearization was recently achieved analytically as part of the Analytical/Numerical Matching (ANM) free wake model which has been previously applied to improve the efficiency and accuracy of time-marching wake dynamics [6,7].

There are some interesting extensions of Periodic Inversion which have not yet been attempted that arise from the linearized description. One is the inclusion of panel methods for blades and bodies in conjunction with the wake dynamics. Source panels, lifting panels, and lifting lines may all be included as a generalization of the linear system, allowing the integrated solution of the coupled wake/blade/body problem, which is presently solved in an uncoupled, iterative manner. Other options arise from representing Periodic Inversion as an equivalent system for Floquet analysis. In this form, the rotor blade dynamics may be included by extension of present Floquet approaches for blade dynamics, again allowing the coupled solution of a

solid/fluid dynamics problem. As the system eigenvalues are available from Floquet analysis, this approach also allows the study of wake stability, which is an issue at low advance ratios. An eigenvalue study may also be done in the present form of a linear algebraic system, although the potential size of the system may make this impractical.

VORTEX WAKE DYNAMICS

Rotor wakes are usually modeled as concentrated regions of vorticity embedded in potential flow. This basic approach is common to the gamut of wake models from momentum theory through prescribed wakes to free wakes. The vorticity is shed from the blade in a sheet extending the full blade span, but this sheet quickly rolls up to form a concentrated filament of vorticity near the blade tip. While vortex sheet elements with two parametric coordinates have been used to model the wake, the simpler vortex filament element with a single parameter has seen much wider use. The obvious application of vortex filaments is to fully developed tip vortices, although vortex sheets and shear layers can also be modeled. A recent approach to modeling full-span wakes uses a system of non-intersecting filaments laid out in constant-strength contours [2]. This approach, illustrated in Figure 1, is physically more consistent than the older approach of modeling a vortex sheet with a lattice of shed and trailed filament elements of varying strength.

The basic goal of free wake calculations is to determine the dynamic evolution of the vortex filaments. The vorticity field evolves along with the material elements of the fluid, convecting with the local fluid velocity in a Lagrangian sense. The velocity arises from two components, the free stream and the induced velocities. The free stream velocity is typically known, but the induced velocity must be repeatedly calculated as it is dependent upon the instantaneous configuration of the wake. The induced velocity at any point is found from integrating the Biot-Savart integral over all of the free and bound vorticity. The Biot-Savart integral is given in Eq. (1) in the form used for vortex filaments.

$$\mathbf{v} = \frac{-\Gamma}{4\pi} \int \frac{\mathbf{r}_v \times d\mathbf{s}}{(r_v^2 + \epsilon^2)^{3/2}} \quad (1)$$

Here $d\mathbf{s}$ is the differential length element along a filament, and ϵ is a vortex core radius discussed below. Vortex filament elements are used to discretize the filament into a piecewise continuous approximation. To facilitate the evaluation of the Biot-Savart integral, the elements are based on simple geometric forms such as parabolas, polynomials, arcs and points. The endpoints of the filament segments are known as collocatio

points, and constitute the discrete set of variables in the wake dynamics calculation. The induced velocities are calculated at the collocation points, and their positions are updated. At each new position, the filament geometry is recomputed by using the collocation points to define the element geometries. Traditionally, the collocation points have been defined as Lagrangian fluid markers, so that their positions are found from the simple kinematic relationship $dx = v dt$. The method of Periodic Inversion modifies this Lagrangian description as discussed at length below.

For a wake consisting of N collocation points, the number of elemental Biot-Savart integrations needed to determine the collocation point velocities at a single instant is of order N^2 . In time marching approaches, wake convergence typically requires order N^3 integrations. Thus computational efficiency is always an issue. There is a hierarchy of vortex elements that generally trade off accuracy for efficiency. The Basic Curved Vortex Element (BCVE) is a very accurate element based on a parabolic fit, but the analytical complexity of the Biot-Savart evaluation makes each element computationally expensive [8,9,10]. Straight line elements are a lower order approximation and are less accurate and less expensive than the BCVE on a per element basis, although since fewer curved elements can be used for comparable accuracy the overall BCVE calculation will still be cheaper. Vortex particles, or "vortons" are the lowest order and least expensive element. The particle velocity is shown in Eq. (2) to be a simple Riemann sum approximation of the Biot-Savart integral.

$$V = \frac{-\Gamma}{4\pi} \sum_i \left(\frac{r_v \times \Delta s}{(r_v^2 + \epsilon^2)^{3/2}} \right)_i \quad (2)$$

Evidence shows that vortex particles compare favorably in accuracy to the BCVE at evaluation distances greater than one element length [7].

The wake model used for Periodic Inversion is based on Analytical/Numerical Matching (ANM), which combines vortex particles with an analytical near-field correction. The ANM model is a recent development in free wake modeling that provides a 500% gain in efficiency over the BCVE model while maintaining a comparable level of accuracy. The ANM model has been previously applied to a time marching wake dynamics code, and compares favorably with the BCVE model [6]. In brief, the inexpensive vortex particles are used alone for the majority of the velocity evaluations. An artificially large core radius ϵ_{fat} is used in (2) to smooth the near-field discretization errors, but the core effect is local so the velocity contributions of points not immediately nearby (effectively the far field) are accurately represented. Points of evaluation in the near

field have their velocities attenuated by the large core and are corrected by an analytical correction with two components. The first component uses a thin core radius ϵ_{thin} corresponding to the physically realistic core size, which can be determined from the blade loading conditions [11]. This thin core component provides the physically correct near field velocity. The second component uses the large core ϵ_{fat} with an opposite sign circulation. In the near field, the large core particle and the opposite sign large core correction cancel, leaving the physically correct thin core velocity. In the far field, the two correction components are made to cancel, leaving the large core particle solution which is accurate in the far field. Thus the ANM method is analogous to matched asymptotic expansions with the thin core correction being the inner solution, the fat core particles being the outer solution, and the opposite sign fat core correction being the matching solution. The ANM approach is illustrated in Figure 2 which shows the composite solution as the sum of the three components. The efficiency of the ANM method results from the bulk of the N^2 elemental velocity calculations being in the far field, where the inexpensive vortex particles are used alone. The analytical correction is only applied for the near-field evaluations, which are order N in number.

Linearization of the elemental velocity expressions with respect to the collocation point variables was necessary to implement Periodic Inversion. This had previously been accomplished during the ANM development to provide added efficiency for time-marching wake calculations [6]. The simple functional form of the vortex particle provided an efficient analytical representation of the Taylor expansion. The near-field analytical correction resulted in a more complicated expansion, but the infrequent application of the correction makes the cost reasonable. All derivatives are found analytically, which is vastly more efficient than numerical derivative calculations.

The upstream end of a wake attaches to the trailing edge of the rotor blades, thus maintaining continuity with the bound vorticity on the rotor surfaces. The downstream end theoretically extends to infinity for steady flight, but in practice the free wake model must be of finite length followed by a semi-infinite prescribed far wake. At high advance ratios, the absence of the extension has a negligible effect, but at low advance ratios and hover the induced velocities of the extensor are important. The ANM model recently incorporated an efficient procedure for including this semi-infinite extension based upon a similar approach developed for the BCVE model [8]. Copies of the last turn of free wake are appended to the free wake as shown in Figure 3. The spacing of the added turns is given by the convection vector r_s , which is an average of the collocation point displacements over the last turn of free wake. Each element in the last turn of free wake thus becomes

semi-infinite row of elements. The ANM far-wake extension uses only the fat core particle contribution, as the uncertainty in the exact extension geometry does not support the use of the thin core near-field correction. The exact velocity induced by a semi-infinite row in the far-field extension is given in Eq. (3).

$$V = \frac{-\Gamma}{4\pi} \sum_{m=0}^{\infty} \frac{(r_v + mr_s) \times \Delta s}{(|r_v + mr_s|^2 + \epsilon^2)^{3/2}} \quad (3)$$

Provided that the distance to the point of evaluation is considerably greater than the element spacing, the sum can be accurately approximated as an integral. This results in the working form of the far-wake extension velocity given in Eq. (4), where M is the finite number of particle velocities used before the integral approximation is applied.

$$V = \frac{-\Gamma}{4\pi} \sum_{m=0}^M \frac{(r_v + mr_s) \times \Delta s}{(|r_v + mr_s|^2 + \epsilon^2)^{3/2}} \quad (4)$$

$$= \frac{-\Gamma}{4\pi} \int_{\frac{M+1}{2}}^{\infty} \frac{(r_v + mr_s) \times \Delta s \, dm}{(|r_v + mr_s|^2 + \epsilon^2)^{3/2}}$$

The far-wake extension does not increase the number of collocation points in the wake, and is essentially a modified element form used for the last turn of free wake. The extension has been analytically linearized consistent with the primary ANM model.

PERIODIC WAKE STRUCTURE

Under general transient flight conditions, a rotor wake is unsteady, and transient solutions must be found by time integration. As such, the collocation point variables $P_i = (px_i, py_i, pz_i)$ may be described as functions of time $P_i(t)$. However, as steady state flight conditions such as hover and steady forward flight are achieved, an ideal solution emerges which is periodic with respect to the azimuthal angle ψ . Assume that the inverse relationship $t = t(\psi)$ is known, which is trivial for the case of constant angular velocity of the rotors. The collocation points may then be described as $P_i(\psi)$. In steady-state flight, a rotor wake is still unsteady in time, but is ideally periodic with respect to the rotor azimuth ψ . Let the coordinate system be nonrotating and fixed at the blade hub. Then for any given value of ψ the collocation points are periodic as:

$$P_i(\psi + n2\pi) = P_i(\psi) \quad (5)$$

$$n = +/- 1, 2, \dots, \infty$$

Eq. (5) represents the periodic boundary conditions necessary for finding the ideal time-independent, steady-state periodic wake structure.

In the above discussion, some liberty was taken in advance to define the collocation points in a non-Lagrangian sense. Since vorticity evolves with material elements in the fluid, the traditional use of collocation points has been as Lagrangian markers, i.e. points on a vortex filament that convect with the fluid. Typically, the filaments are modeled with a finite length, so that at each time step a new Lagrangian collocation point is added at the point where the free vortex separates from the blade. This collocation point convects downstream with the filament over time, and is removed when it reaches the end of the free-wake portion of the filament. As such, the Lagrangian collocation points do not represent a set of variables that behave periodically. After each revolution, the points have convected downstream or have been removed entirely. They do not return to their positions at the previous revolution. It remains to redefine the collocation points as variables with the proper periodic behavior.

In the geometric sense, a vortex filament is described as a space curve of two variables, $R(s,t)$, where s is some general arc length parameter and t is time. In general, collocation points represent discrete locations on the curve at constant values of the arc length parameter as $P_i(t) = R(s_i, t)$. The Lagrangian collocation points may be defined at values of the specific parameterization $R(s_L, t)$, where s_L physically corresponds to the time that the collocation points are introduced at the upstream end of the filament. This will be referred to as the Lagrangian parameterization. It is now possible to define a new parameter defining the age of a Lagrangian collocation point as $s_A = t - s_L$, which is the difference between the current time and the time that the point was introduced into the fluid. Thus s_A will be defined as the age parameter. Note that a vortex filament has a constant range of age, s_A , starting at zero at the blade and increasing to some maximum value defined by its length, and that each Lagrangian point varies in age over this full range. A periodic set of variables can be defined by using age as the arc length parameter $R(s_A, t)$. A collocation point defined at a constant age value, $P_i(t) = R(s_{A_i}, t)$, does return to the same location each period under steady-state conditions. For example, a point with a constant age of zero will always be located at the blade release point, and will return with the blade to the same position at each revolution. It is these constant-age collocation points, not the Lagrangian collocation points, that were

used in the discussion of Eq. (5). The relationship between the two descriptions is illustrated in Figure. 4.

A further parametric generalization which has not yet been attempted is worth mention. It appears possible to define an arc length parameter that is periodic and also allows local element refinement. Element refinement refers to increasing the vortex element density in regions where the added resolution is required, and is analogous to local mesh refinement in grid-based CFD methods. For example, in forward flight the advancing and trailing sides of the wake ($\psi=90,270$) are characterized by strong vortex roll-up, while the central portion of the wake ($\psi=0,180$) is relatively benign. Increasing the element density on the advancing and trailing sides could lead to solution efficiencies with respect to maintaining overall consistency in the accuracy. For illustration, such refinement can be achieved by the following parametric generalization:

$$s_G = s_A + a \sin(2 \Omega s_A) \quad (6)$$

where Ω is the blade angular velocity and a is a constant defining the strength of the local refinement.

One further aspect of periodic wakes is the symmetry introduced by multiple blades. As a result of the wake being in a periodic steady-state condition, the wake trailed from each blade is a phased copy of all other blade wakes. Given B blades uniformly spaced around the hub, the wake can be exactly defined by $1/B$ blade revolutions. Thus, to describe a single-blade wake, 360° of azimuth are required. Extending the model to two blades doubles the number of vortex elements, but halves the interval needed to 180° of azimuth. Using the multi-blade symmetry results in the solution time increasing only linearly with the number of blades.

PERIODIC INVERSION METHOD

The basic descriptions for both periodic inversion and traditional time marching come from the total time derivative of the parametric filament description $R(s,t)$ given by:

$$\frac{dR}{dt} = \frac{\partial R}{\partial s} \frac{ds}{dt} + \frac{\partial R}{\partial t} \quad (7)$$

where the total derivative dR/dt is the Lagrangian velocity V as found by the Biot-Savart law. For the Lagrangian parameterization, $ds/dt = 0$ and Eq. (7) reduces to the simple kinematic relationship $dR = V dt$ which is the basis for time-marching integration approaches. In the age parameterization, $ds_A/dt = 1$ and Eq. (7) becomes:

$$\frac{dR_i}{dt} = \frac{\partial R_i}{\partial s_A} + \frac{\partial R_i}{\partial t} \quad (8)$$

where $\partial R/\partial s_A$ represents evolution tangent to the filament, and $\partial R/\partial t$ is non-Lagrangian convective evolution. The subscript index i represents the filament discretization into the collocation point variables. Note that if the induced (Biot-Savart) velocity is zero, Eq. (8) becomes the one-dimensional wave equation that simply describes the propagation of a disturbance along the filament.

The filament is now written in the form $R(s_A,t) = R_0(s_A,t) + r(s_A,t)$, where $R_0(s_A,t)$ is prescribed over a full period, and $r(s_A,t)$ is a perturbative correction to be found. Further, expand the velocity V about R_0 to linear order in a Taylor series with respect to the collocation points. Making these substitutions in Eq. (8) and collecting the known terms on the right hand side results in the following expression:

$$\frac{\partial r_i}{\partial s_A} + \frac{\partial r_i}{\partial t} - \sum_{k=1}^N \frac{\partial V_i}{\partial R_{0k}} r_k = V_{0i} - \left(\frac{\partial R_{0i}}{\partial s_A} + \frac{\partial R_{0i}}{\partial t} \right) \quad (9)$$

where the summation is over all collocation points at a specific instant in time. Equation (9) describes the instantaneous wake velocity. It is a linearized approximation to Eq. (8), where the nonlinearity arose from the Biot-Savart velocity. The wake is discretized in both the temporal and spatial coordinates. Temporal discretization is achieved by dividing the rotor period into a number of intervals, typically of equal azimuthal increments. Spatial resolution regards the number of elements or collocation points used to describe each vortex filament. Equation (9) is evaluated at each azimuthal increment. The velocity and its derivatives are calculated from the Biot-Savart law applied to the prescribed filament at that azimuth, and the partial derivatives are approximated using finite differencing which couples the temporal intervals. Applying the periodicity condition (5) results in a closed linear system of the form $Ar = b$. A simple example of this is found by considering the first order equation with a periodic boundary condition given in Eq. (10). Using three intervals over the period T and backward differencing for the derivative term results in the closed linear system shown in Eq. (11).

$$\dot{x} + f(t)x = g(t), \quad x(t+T) = x(t) \quad (10)$$

$$\begin{bmatrix} 1+f^1\Delta t & 0 & -1 \\ -1 & 1+f^2\Delta t & 0 \\ 0 & -1 & 1+f^3\Delta t \end{bmatrix} \begin{bmatrix} x^1 \\ x^2 \\ x^3 \end{bmatrix} = \begin{bmatrix} g^1\Delta t \\ g^2\Delta t \\ g^3\Delta t \end{bmatrix} \quad (11)$$

As Eq. (9) is a linear approximation to a nonlinear problem, iterative refinement is necessary to achieve satisfactory convergence. The solution proceeds by improving the prescribed wake as $R_0^{(n+1)} = R_0^{(n)} + r^{(n)}$ where the perturbative correction is found from $r^{(n)} = A^{-1(n)}b^{(n)}$. The periodicity condition (5) ensures that each iteration results in a periodic structure. The vector b is a measure of residual, and $\|b\| \rightarrow 0$ at convergence, which can be seen by recognizing that the terms on the right of Eq. (9) are from the total derivative of the prescribed wake R_0 .

NUMERICAL IMPLEMENTATION

The implementation of the periodic inversion approach involves two general topics: the specific numerical methods used to solve the problem, and the programming considerations. The numerical methods define the evaluation of the velocity terms in Eq. (9), the finite differencing approach used to generate the coefficient arrays A and b , and the solution of the resulting linear system. The velocity V_0 and its derivative $\partial V/\partial R_0$ are functions of the vortically induced velocity, although V_0 also includes the constant free-stream velocity. For each azimuthal step in the period, the prescribed wake R_0 is used to define the instantaneous wake configuration. Specifically, the ANM method described earlier is used for the evaluation of the velocity and velocity derivatives.

The finite differencing scheme used must be consistent with the hyperbolic nature of Eq. (8). Further, it should be chosen to provide an advantageous structure for the coefficient matrix A . The internal structure of A affects both the storage requirements and the solution procedure used for its inversion, which are important considerations due to the potential size of the linear system. The scalar rank of A is given by $(3*N*K)/B$, where N is the number of vortex elements in the wake, B is the number of blades, and K is the number of azimuthal steps per period. For example, a two-bladed rotor trailing tip vortices with five turns of free wake each using a 10° step size would result in nearly 20,000 simultaneous equations, and could require almost 400,000,000 array elements if A were full (fortunately it is not).

With two exceptions, the finite difference scheme used at the collocation points is the Lax-Wendroff method [12, p.101] which is second-order accurate in both space and time. The velocity terms are treated as the average between the two time steps used for the derivative terms, which represents trapezoidal integration of the velocity. The resulting difference equation for (9) is given in Eq. (12), where the CFL number is given by $v = \Delta t/\Delta s_A$.

$$r_i^n = r_i^{n-1} - \frac{v}{2} (r_{i+1}^{n-1} - r_{i-1}^{n-1}) + \frac{v^2}{2} (r_{i+1}^{n-1} - 2r_i^{n-1} + r_{i-1}^{n-1}) - \left[R_{0i}^n + \frac{v(1-v)}{2} R_{0i+1}^{n-1} + (v^2-1) R_{0i}^{n-1} - \frac{v(v+1)}{2} R_{0i-1}^{n-1} \right] + \frac{\Delta t}{2} \sum_{k=1}^N \left[\frac{\partial V_i^n}{\partial R_{0k}^n} r_k^n + \left(v \frac{\partial V_{i-1}^{n-1}}{\partial R_{0k}^{n-1}} r_k^{n-1} + (1-v) \frac{\partial V_i^{n-1}}{\partial R_{0k}^{n-1}} r_k^{n-1} \right) \right] + \frac{\Delta t}{2} [V_{0i}^n + (vV_{0i-1}^{n-1} + (1-v)V_{0i}^{n-1})] \quad (12)$$

The first exception is the first collocation point on each filament. This point is assumed fixed to the blade, so that its kinematic motion is prescribed and provides a boundary condition. The second exception is the last point on each filament. An upwind difference scheme from Warming and Beam is used which is also second-order accurate [12, p.103]. The resulting equation is given in Eq. (13).

$$r_i^n = r_i^{n-1} - v (r_i^{n-1} - r_{i-1}^{n-1}) + \frac{v(v-1)}{2} (r_i^{n-1} - 2r_{i-1}^{n-1} + r_{i-2}^{n-1}) - \left[R_{0i}^n + \frac{(2-v)(v-1)}{2} R_{0i}^{n-1} + v(v-2) R_{0i-1}^{n-1} - \frac{v(v-1)}{2} R_{0i-2}^{n-1} \right] + \frac{\Delta t}{2} \sum_{k=1}^N \left[\frac{\partial V_i^n}{\partial R_{0k}^n} r_k^n + \left(v \frac{\partial V_{i-1}^{n-1}}{\partial R_{0k}^{n-1}} r_k^{n-1} + (1-v) \frac{\partial V_i^{n-1}}{\partial R_{0k}^{n-1}} r_k^{n-1} \right) \right] + \frac{\Delta t}{2} [V_{0i}^n + (vV_{0i-1}^{n-1} + (1-v)V_{0i}^{n-1})] \quad (13)$$

The apparent complexity of Eqs. (12) and (13) hides some simple rewards. When $v = 1$, the Lagrangian and constant age collocation points are coincident, with one point being added for each azimuthal increment of the blade. In this case, the truncation errors of both difference schemes are zero and no dispersion or dissipation error is introduced. Also for $v = 1$, in the absence of a velocity field, both (12) and (13) reduce to $R_{0j}^n + r_j^n = R_{0j-1}^{n-1} + r_{j-1}^{n-1}$, which simply represents the propagation of a disturbance along the filament, recovering the solution to the linear wave equation.

This difference scheme results in the coefficient matrix A having a periodic block bi-diagonal structure, which is analogous to the form shown in Eq. (11) with the scalar elements replaced by block matrices. The main diagonal and lower diagonal blocks are fully populated, as is the upper right corner block, while the remaining blocks are zero. Each row of blocks corresponds to one azimuthal rotor step. The sparsity of the matrix results in an array storage requirement of $(18*K*N^2)/B$, which for the previous example would result in roughly

40,000,000 elements, about an order of magnitude less than if A were full. The linear system is solved using a modification of PBTRIP, a subroutine developed for the solution of periodic block tri-diagonal systems without a pivoting strategy [12, p.551]. The modification removed the usage of the upper diagonal blocks, which reduced the array size and improved the execution speed. However even though the matrix is sparse and an efficient solution procedure is available, the size of the system can be formidable even for supercomputers. A possible future effort will be to re-cast the problem in terms of a Floquet analysis rather than as a linear system of equations. This would have three benefits. First, the size of the problem would be reduced from $(3*N*K)/B$ linear equations to $3*N$ coupled ODE's, at the expense of calculating a time-dependent coefficient matrix for the Floquet analysis. Second, the eigenvalues of the linearized problem are readily found from the Floquet solution, allowing the opportunity to study the stability of wake solutions at low advance ratios and hover. Third, Floquet analysis is used in studying blade structural dynamics [13]. This invites the integrated coupling of the solid and fluid mechanics of the overall aeroelastic problem.

The program written for Periodic Inversion represents about 10,000 lines of FORTRAN, roughly half of which are comments. Half of the program is the linearizing ANM code which is in the form of a modular library, and which is also used by a time-marching wake dynamics code. The program was developed under a UNIX environment, and is being run on a Cray Y-MP at the North Carolina Supercomputing Center. The primary program task is to converge a wake for a specific set of performance variables such as advance ratio μ , thrust coefficient C_t , and tip path plane angle TPP. This inner convergence loop repeatedly iterates the solution in the manner described in the previous section. Convergence is defined as a maximum allowable rms displacement of all collocation points between two successive iterations. The solution can be used as an initial condition for restarts at different flight conditions, or as an initial condition for time-marching studies for comparison of the methods.

The generation of performance curve data is an advantage of periodic inversion, and an outer loop of the program allows the solution to follow a performance curve. By selecting points on the performance curve which are linearly close together, converged wakes at each point can be found with one or very few periodic inversions. At present μ , C_t and TPP can be simultaneously varied in a prescribed manner. The program maintains an active control over the variable step sizes. If the solution at a new point is not converging, the step size is reduced and the solution at a closer point on the curve is started. Also, if the solution is converging rapidly at several concurrent

points, a larger step size is attempted to speed the overall curve generation.

RESULTS

To illustrate the method, a rotor wake was converged at hover, and then the advance ratio was increased into the range of low speed flight where time-marching approaches are applicable. The model used two tip vortices to approximate the wake of a twin-bladed rotor with a 20 ft. radius revolving at 286 rpm. Each filament extended for four turns of free wake using 24 elements per turn (15° azimuthal spacing). This resulted in 194 collocation points, 6985 simultaneous equations, and required 8.13 Mword of storage for A . The initial convergence at hover was achieved by starting at a low thrust coefficient of $C_t = 0.001$ and then increasing it at hover to the final value of $C_t = 0.003$, which was then held constant as the advance ratio increased. The tip path plane angle was defined as $TPP = 100*\mu$ (in degrees) so that at $\mu = 0.05$, $TPP = 5^\circ$. The specific performance curve followed is given in Figure 5, which indicates the individual points found on the curve. The small step sizes in the range $0.025 < \mu < 0.03$ were required by the rapid change in the wake in this region as discussed below. Convergence at each performance point was defined by an rms collocation point displacement between iterations of less than 0.05% of the rotor radius.

The advance from hover to forward flight is illustrated in Figures 6 to 13, which show isometric views of the wake. The far-wake extension is shown appended to the last turn of free wake, which is why the wake does not appear to evolve downstream of the fourth turn. However, at any advance ratio except hover, the wake does continue to evolve downstream into a diffuse vortex pair similar to the contrails of fixed-wing aircraft. The computational burden of capturing this convolution places a practical limit on the number of turns of free wake that can be modeled. Even so, the correct behavior is apparent at the higher advance ratios which show the roll-up along the advancing and retreating edges of the wake. It should be noted that the same results were found in the opposite direction by reducing the advance ratio from forward flight to hover.

For the range $0 < \mu < 0.025$, the wake is approximately a skewed helix, but a distinct transformation occurs for $0.025 < \mu < 0.03$ as the roll up on the advancing and retreating sides develops rapidly. Above $\mu = 0.03$ the roll up is essentially developed and further changes are in large due to the free stream convecting the wake further behind the rotor disk. The specific transition values of μ will in general depend on the thrust coefficient and other wake parameters. Due to the nonlinearity of the problem it is interesting to speculate on the number, stability, and uniqueness of

solutions. The roll up may represent a transition from an increasingly unstable "helical" structure to a more stable configuration. It is interesting to note that several other twin-bladed wake models were attempted with variations in the free-wake length, element density and thrust coefficient. They all required fine time steps near this transition region, suggesting that the rapid transition to roll-up is physically correct. Certainly the transition must occur to evolve the wake from the symmetry of hover to the familiar roll-up of forward flight, although the abruptness of the transition is surprising.

Given the possibility of several solutions to a nonlinear system, it must be questioned if the ones found by Periodic Inversion are unique and physically meaningful. An exhaustive answer to this issue would involve a comprehensive parameter study and stability analysis, which is beyond the present scope. Some promising evidence that the solutions are unique is provided by checking the results with time-marching solutions of the same wake model. The solutions found by Periodic Inversion at several intermediate advance ratios were used as initial conditions for time marching solutions, which were allowed to integrate the solution for 40 blade revolutions to examine the convergence behavior. To converge, time-marching typically needs to proceed through slightly more revolutions than the number of turns of free wake. Thus 40 revolutions were chosen to conservatively test the stability of the time-marching solutions. The convergence results are given in Figure 14, which presents the rms difference of the collocation points between the initial condition from the periodic solution and the value found by time marching after each revolution. At advance ratios above the transition region ($\mu > 0.03$), the time-marching solutions reach a steady state which is essentially the same as found by Periodic Inversion. The small but constant rms difference is attributable to the different numerical schemes of the two approaches. The solution within the transition region ($\mu \approx 0.025$) is seen to oscillate about the periodic solution with increasing amplitude as the integration proceeds, and is tending toward divergence at the end of the run. The solution at $\mu = 0.02$ is below the transition region and also oscillates about the periodic solution for roughly 10 revolutions, but then rapidly diverges. These results suggest three things: first, that the periodic and time-marching solutions are essentially identical at advance ratios above the roll-up transition. Second, the helical wake structures below the transition region are correct in the mean sense. They provide a wake configuration about which the transient solution oscillates before being overwhelmed by the perturbations. Finally, this reinforces the idea that the helical structure is less stable than the post-transition roll-up structure, providing a quantitative lower limit for the application of time-marching solutions.

CONCLUSIONS

A new approach for the calculation of rotor free wakes has been developed which guarantees periodically steady-state solutions by enforcing periodic boundary conditions over $1/B$ rotor revolutions, where B is the number of rotor blades. The method is based on developing a system of collocation points with periodic behavior, as opposed to the Lagrangian description used in time-marching approaches. The vortically induced velocities determined from the Biot-Savart law are linearized, and the wake dynamics over a full period are written in a linear perturbation form. The recently developed Analytical/Numerical Matching (ANM) wake model is used to define the discrete wake model. The ANM model has been analytically linearized providing a straight-forward extension to Periodic Inversion. A new far-wake extension, which accounts for the semi-infinite domain of the wake, has been developed for this method and incorporated into the ANM model. The resulting problem takes the form of a large linear system of algebraic equations which is inverted for the perturbative correction vector. As this is a linear approximation to a nonlinear problem, iterative refinement is typically required to reach convergence.

A primary advantage of Periodic Inversion is that it provides the means to study wake dynamics at all advance ratios, including hover. Low advance ratios have previously been unattainable for traditional time-marching approaches due to poor convergence behavior. The new method has shown that the wake maintains a roughly helical structure from hover up to some lower bound on the advance ratio. As the advance ratio is increased from this lower bound through a narrow transition region, the wake quickly evolves into the familiar roll-up configuration characteristic of forward flight. At advance ratios above the transition region, the wake maintains the roll-up form and does not qualitatively change. Comparison with time-marching solutions show excellent agreement for wakes above the roll-up transition. Wakes within and below the transition region prove difficult for time-marching to converge, but there is evidence that the periodic solution provides a correct mean wake structure about which time-marching solutions oscillate.

Periodic Inversion also provides the means to generate performance curve data. Wake variables such as advance ratio, thrust coefficient and tip path plane angle can all be varied between iterations of the method. Points on a performance curve which are linearly close together can be incrementally found with one or very few iterations. This approach was used in the present study for two purposes. First, the wake was converged at hover by incrementing the thrust coefficient from 0.001 to 0.003. The thrust coefficient was then held constant as the advance ratio and tip path plane angle were

increased. The pre- and post-transition range of the advance ratio were easily solved with a fairly large step size. Within the transition region, a much finer step size was required to capture the rapid change in the wake structure. Future work should address the robustness of the method in this region, as well as investigate the general character of the solution stability.

There are unique and promising opportunities for further extensions of the method. A generalization of the periodic variable description will allow the vortex element density to be increased in regions of strong vortex interactions, such as the advancing and retreating side roll up. This will allow a more efficient overall wake model without compromising accuracy. Coupling the wake dynamics with blade and body panel methods will allow an integrated approach to include both blade lift and interactional aerodynamics. This results from the generalization of the linear system to include the lifting and non-lifting body panel equations. It appears possible to incorporate the blade dynamics into the method as well.

ACKNOWLEDGEMENT

This research was sponsored by a Fellowship from NASA-Ames under the Graduate Student Researchers' Program and a grant from the U. S. Army Research Office. Computing resources were provided by the North Carolina Supercomputing Center.

REFERENCES

1. Hooper, W. E., "The Vibratory Loading of Helicopter Rotors," Paper No. 46, 9th European Rotorcraft Forum, Stresa, Italy, September 13-15, 1983.
2. Bliss, D. B., Dadone, L., and Wachspress, D. A., "Rotor Wake Modeling for High Speed Applications," Proc. of the 43rd Annual Forum of the American Helicopter Society, May 1987.
3. Egolf, T. A., "Helicopter Free Wake Prediction of Complex Wake Structures Under Blade Vortex Interaction Conditions" Proc. of the 44th Annual Forum of the American Helicopter Society, Washington, DC, June 1988.
4. Quackenbush, T. R., "Computational Studies in Low Speed Rotor Aerodynamics," Ph.D. Thesis, Dept. of Mechanical and Aerospace Engineering, Princeton University, Princeton, NJ, Oct. 1986.
5. Bliss, D. B., Wachspress, D. A., and Quackenbush, T. R., "A New Approach to the Free Wake Problem for Hovering Rotors," Proc. of the 41st Annual Forum of the American Helicopter Society, May 1985.
6. Bliss, D. B., and Miller, W. O., "Efficient Free Wake Calculations Using Analytical/Numerical Matching and Far-Field Linearization," Proc. of the 45th Annual Forum of the American Helicopter Society, Boston, MA, May 1989.
7. Bliss, D. B., and Miller, W. O., "Vortex Filament Calculations by Analytical/Numerical Matching with Comparison to Other Methods," Presented at the AIAA 9th Computational Fluid Dynamics Conference, Buffalo, NY, June 13-15, 1989.
8. Bliss, D. B., Teske, M. E., and Quackenbush, T. R., "A New Methodology for Free Wake Analysis Using Curved Vortex Elements," NASA CR 3958, Dec. 1987.
9. Bliss, D. B., Teske, M. E., and Quackenbush, T. R., "Free Wake Calculations Using Curved Vortex Elements," Proceedings of the International Conference on Rotorcraft Basic Research, sponsored by ARO and the Amer. Helicopter Soc., Research Triangle Pk., NC, Feb. 1985.
10. Bliss, D. B., Quackenbush, T.R. and Bilanin, A.J., "A New Methodology for Helicopter Free Wake Analyses," paper A-83-39-75-000, presented at the 39th Annual Forum of the American Helicopter Society, St. Louis, Missouri, May 1983.
11. Bliss, D. B., "Prediction of Tip Vortex Self-Induced Motion Parameters in Terms of Rotor Blade Loading," Proceedings of the American Helicopter Society National Specialists' Meeting on Aerodynamics and Aeroacoustics, Arlington, TX, Feb. 1987.
12. Anderson, D. A., Tannehill, J. C., and Pletcher, R. H., Computational Fluid Mechanics and Heat Transfer, Hemisphere Publishing Corporation, McGraw-Hill Book Company, New York, 1984.
13. Johnson, W., Helicopter Theory, Princeton University Press, Princeton, NJ, 1980.

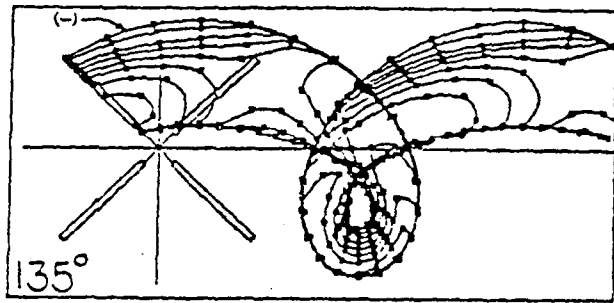


Figure 1: Full span rotor wake modeled with constant strength vortex filaments

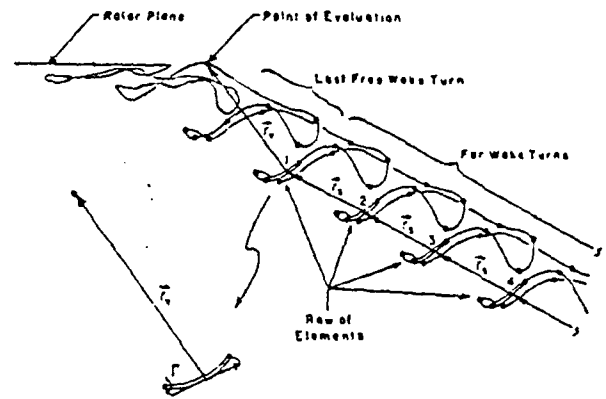


Figure 3: ANM far-wake extension model

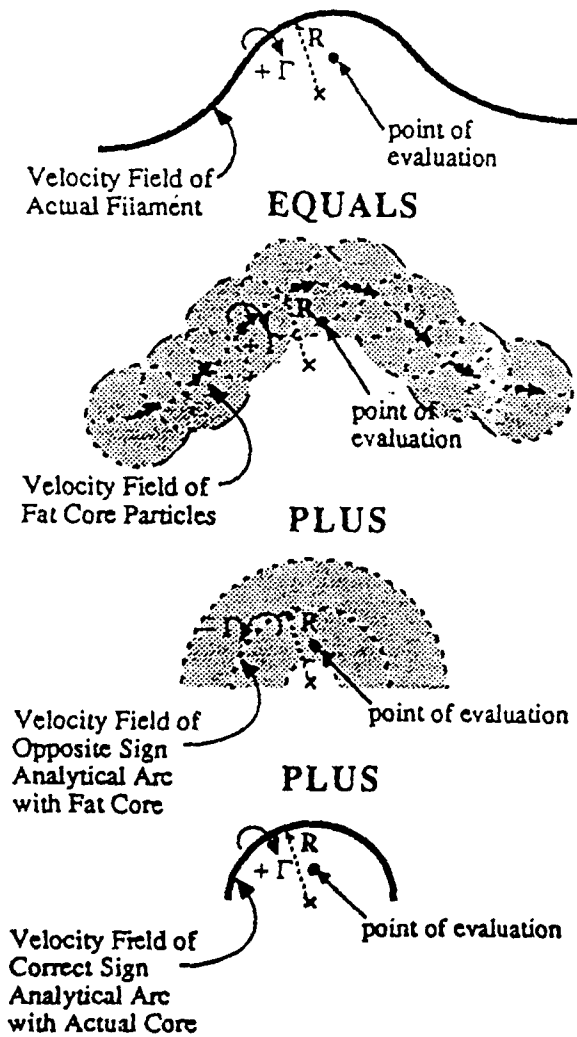


Figure 2: Schematic representation of the ANM.wake model used for time marching and Periodic Inversion.

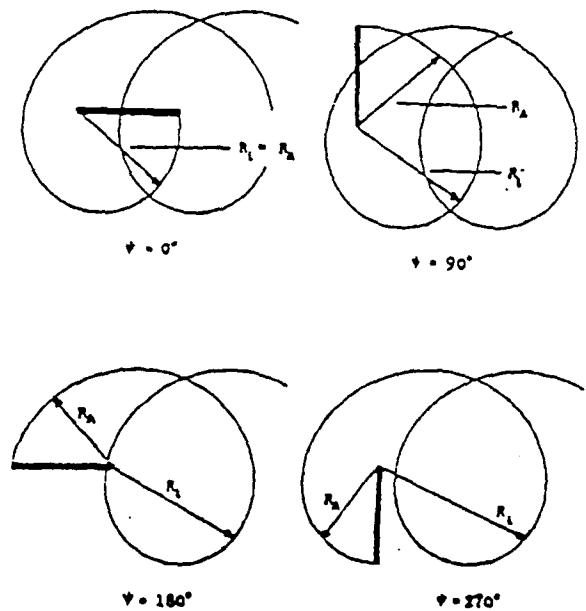


Figure 4: Comparison of constant age vs. Lagrangian collocation points.

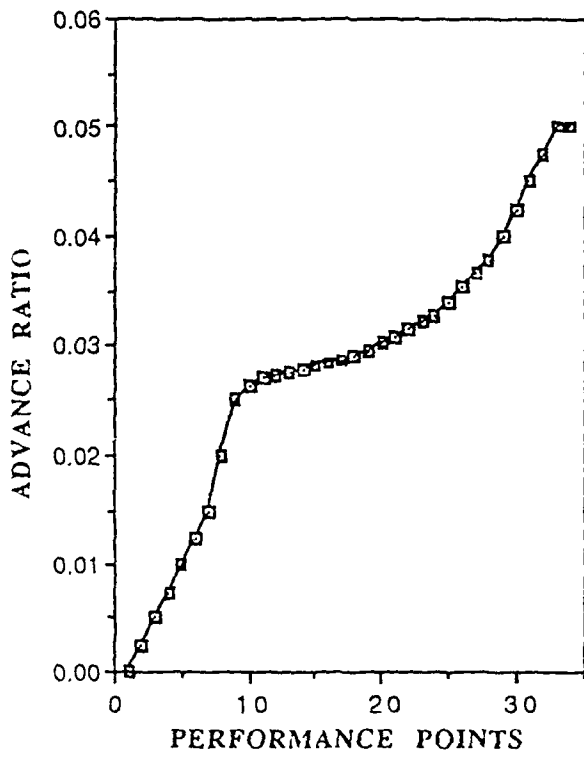


Figure 5: Performance curve used to follow wake evolution from hover to $\mu = 0.05$.

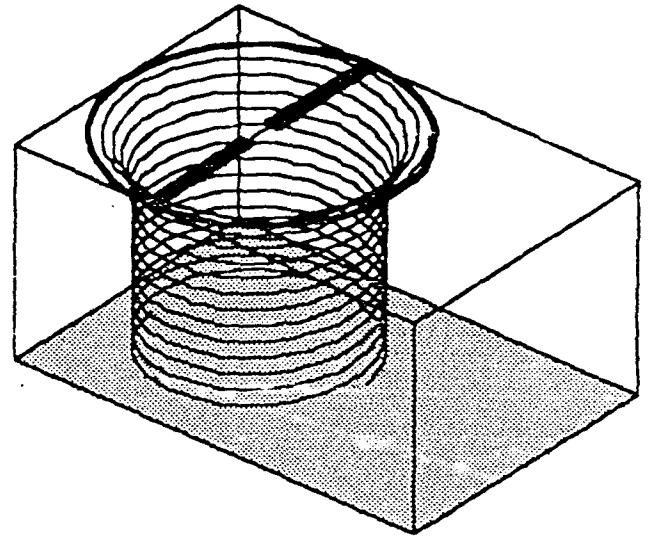


Figure 6: Periodic wake at $\mu = 0.0$

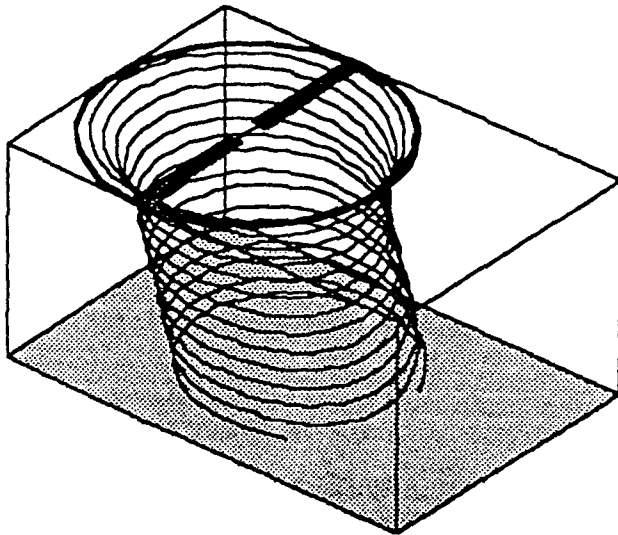


Figure 7: Periodic wake at $\mu = 0.01$

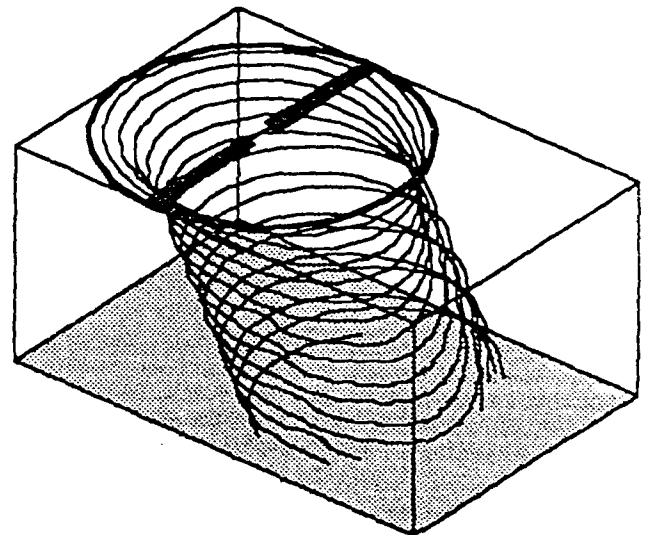


Figure 8: Periodic wake at $\mu = 0.02$

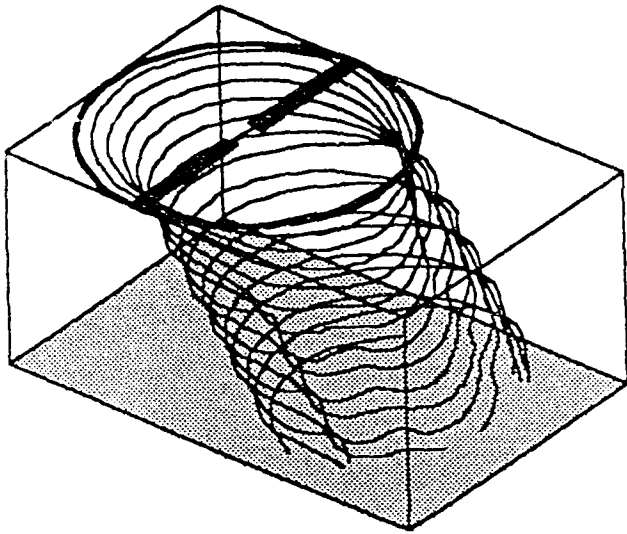


Figure 9: Periodic wake at $\mu = 0.025$

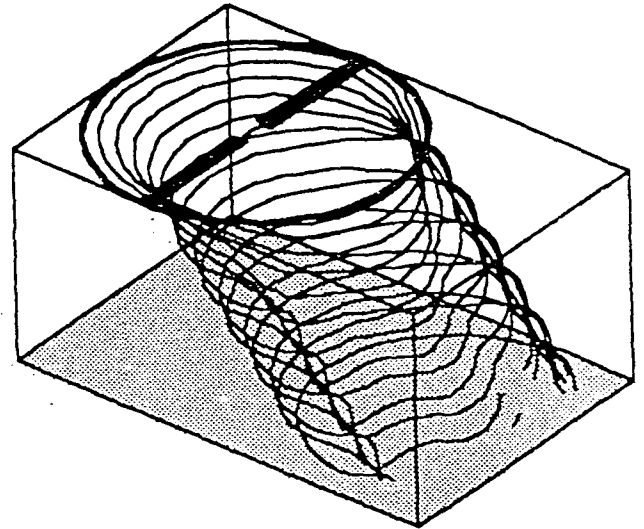


Figure 10: Periodic wake at $\mu = 0.0275$

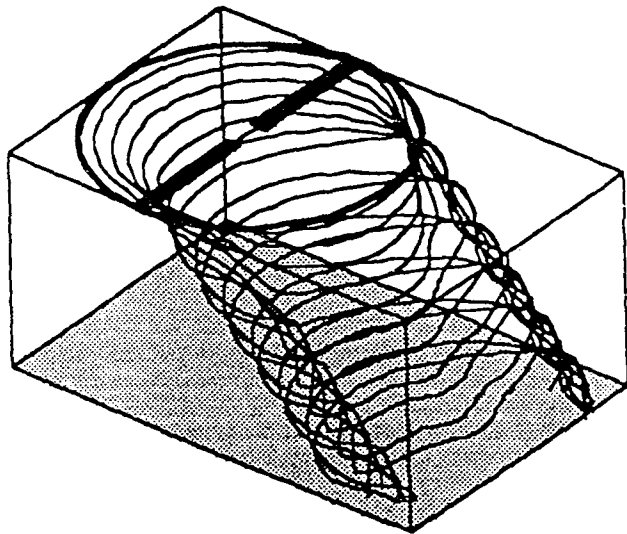


Figure 11: Periodic wake at $\mu = 0.03$

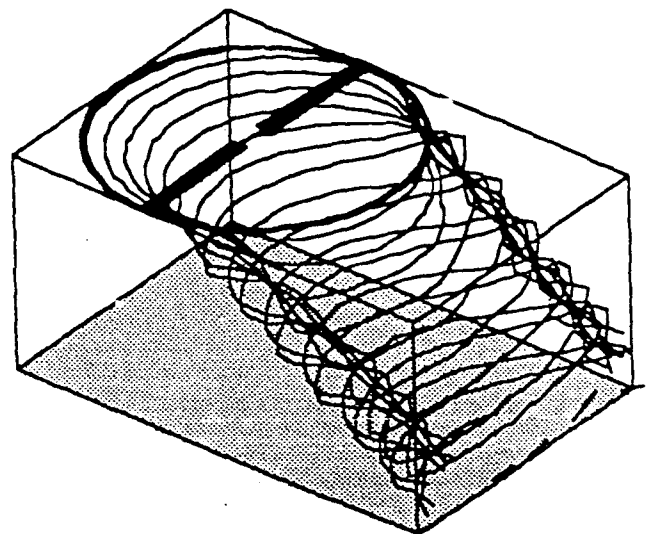


Figure 12: Periodic wake at $\mu = 0.04$

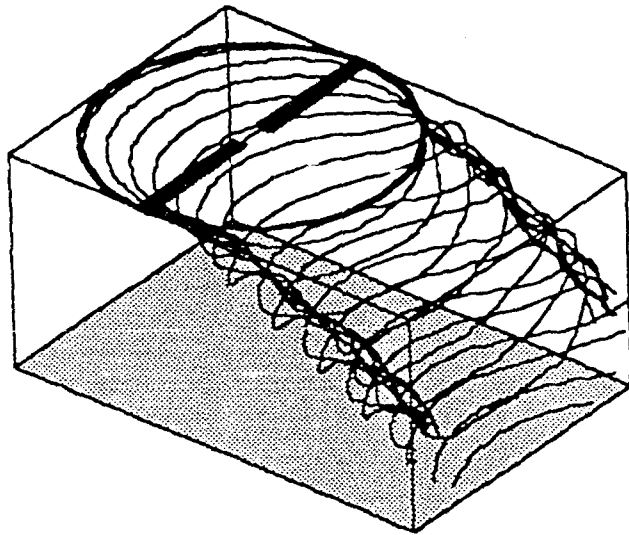


Figure 13: Periodic wake at $\mu = 0.05$

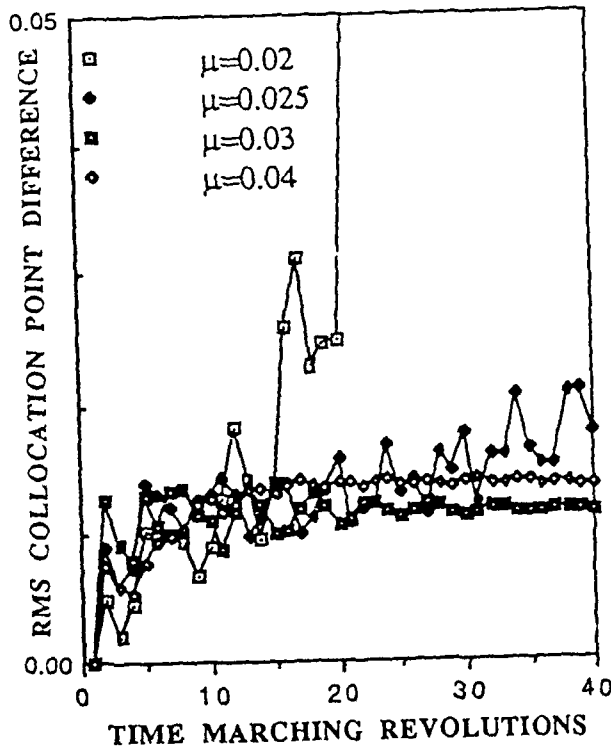


Figure 14: RMS convergence history of time-marching wake dynamics with respect to periodic solution.